ELSEVIER

Contents lists available at ScienceDirect

Journal of Hazardous Materials

journal homepage: www.elsevier.com/locate/jhazmat





Dissolved organic matter production from herder application and in-situ burning of crude oil at high latitudes: Bioavailable molecular composition patterns and microbial community diversity effects

Patrick L. Tomco^{a,*}, Khrystyne N. Duddleston^b, Adrienne Driskill^a, Jasmine J. Hatton^b, Kirsten Grond^b, Toshia Wrenn^a, Matthew A. Tarr^c, David C. Podgorski^{a,c,d,e}, Phoebe Zito^{a,c,d}

- ^a Department of Chemistry, University of Alaska Anchorage, 3211 Providence Dr., Anchorage, AK 99508, USA
- b Department of Biological Sciences, University of Alaska Anchorage, 3211 Providence Dr., Anchorage, AK 99508, USA
- ^c Department of Chemistry, University of New Orleans, New Orleans, LA 70148, USA
- d Chemical Analysis & Mass Spectrometry Facility, University of New Orleans, New Orleans, LA 70148, USA
- e Pontchartrain Institute for Environmental Sciences, Shea Penland Coastal Education and Research Facility, University of New Orleans, New Orleans, LA 70148, USA

ARTICLE INFO

Editor: Dr. R. Maria Sonia

Keywords:
ISB Oil Spill mitigation at high latitudes
Siltech OP-40 Chemical Herder
FT-ICR MS
Ultrahigh resolution mass spectrometry
PARAFAC fluorescence spectroscopy
16S
rRNA gene sequencing

ABSTRACT

Chemical herders and in-situ burning (ISB) are designed to mitigate the effects that oil spills may have on the high latitude marine environment. Little information exists on the water solubilization of petroleum residues stemming from chemically herded ISB and whether these bioavailable compounds have measurable impacts on marine biota. In this experiment, we investigated the effects of Siltech OP40 and crude oil ISB on a) petroleum-derived dissolved organic matter (DOM $_{\rm HC}$) composition and b) seawater microbial community diversity over 28 days at 4 $^{\circ}$ C in aquarium-scale mesocosms. Ultra-high resolution mass spectrometry and fluorescence spectroscopy revealed increases in aromaticity over time, with ISB and ISB+OP40 samples having higher % aromatic classes in the initial incubation periods. ISB+OP40 contained a nearly 12-fold increase in the number of DOM $_{\rm HC}$ formulae relative to those before ISB. 16S rRNA gene sequencing identified differences in microbial alpha diversity between seawater, ISB, OP40, and ISB+OP40. Microbial betadiversity shifts were observed that correlated strongly with aromatic/condensed relative abundance and incubation time. Proteobacteria, specifically from the genera *Marinomonas* and *Perlucidibaca* experienced -22 and +24 log $_2$ -fold changes in ISB+OP40 vs. seawater, respectively. These findings provide an important opportunity to advance our understanding of chemical herders and ISB in the high latitude marine environment.

1. Introduction

Oil and gas drilling has occurred in Alaska since the 1950s, with additional lease sales planned for Cook Inlet and the Beaufort Sea. As regions in the Arctic become ice-free, offshore drilling in that area is expected to increase. As petroleum development increases so does the risk of another major oil spill. The common response to an accidental maritime oil spill typically involves mechanical (boom and skimmer) and/or chemical (dispersants or herders) tools; however, the "appropriate response" arsenal is one that is dynamically employed and depends on a variety of potential recovery tools specifically targeted to the environmental conditions, hydrocarbon characteristics, and relative toxicity of these techniques towards sensitive aquatic organisms. In a

remote Arctic scenario where response times can be long and mechanical tools may not be efficacious in ice-associated areas, *in-situ* burning (ISB) is a popular method to remove oil mass (Fritt-Rasmussen et al., 2015). Burn efficiency can be optimized with use of surface collection agents, "herders" (Buist et al., 2011).

Chemical herders are surfactants applied around the perimeter of an oil spill. The herder forms a monolayer on the surface of the water, forcing the oil to concentrate into a thicker slick that can be ignited (Buist et al., 2018). Siltech OP-40 (CAS number 67674-67-3) is a popular herder formulation included in the U.S. EPA National Contingency Plan Product Schedule that is approved for use in cold regions (USEPA, 2021). The formulation is a renamed version of Silsurf A004-UP, a silicone-based polyether formulation (80% w/w) (Fingas, 2013). This

^{*} Corresponding author at: 3211 Providence Dr., Anchorage, AK 99508, USA. *E-mail address*: pltomco@alaska.edu (P.L. Tomco).

formulation is effective in herding oil for combustion in both ice-free and ice-associated environments (Buist et al., 2011, 2018, 2006, 2008, 2010b, 2010a; Buist and Morrison, 2005; Rojas-Alva et al., 2020).

Once petroleum enters the marine aquatic environment, biotic and abiotic degradation processes can transform its chemical and physical properties. Temporal weathering processes can alter the composition of petroleum making it more complex (Aeppli et al., 2012, 2013; McKenna et al., 2013). Changes in solubility that coincide with these transformations as petroleum-derived residues weather, can result in the production of petroleum-derived dissolved organic matter (DOM_{HC}). DOM_{HC} encompasses the entire range of bioavailable compounds, including both parent and "dead-end" transformation products (Essaid et al., 2011; Bekins et al., 2016; Zito et al., 2019b). Due to dissolution, DOM_{HC} may be distributed throughout aquatic environments once it is mobilized because of dissolution. Determining the chemical character of these highly bioavailable compounds is critical as they are responsible for exposure to marine aquatic organisms that may not come in direct contact with burn residue. The ability to profile DOM_{HC} is an emerging area of study and is viewed as highly relevant to aquatic toxicity (Fingas, 2017). Differences in chemical composition of petroleum transformation products have been shown to inhibit bioluminescence of microtox algae (Zito et al., 2019b; Podgorski et al., 2018; McGuire et al., 2018; King et al., 2014); however, a major research gap that currently exists is in linking chemical character of ISB-derived DOM_{HC} to toxicity effects on exposed organisms collected from the local environment. To date, little information exists with respect to DOM_{HC} resulting from herded ISB oil. The formation of partially oxidized, water-soluble compounds from petroleum with relatively high O/C is consistent with previous reports on in-situ burning and photooxidation of Macondo crude oil associated with the Deepwater Horizon blowout (Zito et al., 2019b, 2020; Jaggi et al., 2019; Bianchi et al., 2014; Ray et al., 2014).

Oil degrading microbes are active in most, if not all arctic and subarctic marine conditions that may be encountered in Alaska waters, including marine sediments (Dong et al., 2015; Wang et al., 2008), ocean water (McFarlin et al., 2014; Prince et al., 2013; Gallego et al., 2014), and pack ice (Brakstad et al., 2008; Gerdes et al., 2005). Often, a few characteristic genera of oil degraders are common (e.g., Cycloclasticus, Alkanivorax), but the suite of microbes, particularly the consortia required to decompose oil constituents beyond their primary metabolites (Bao et al., 2012), remains a major research topic today. Microbial diversity has been assessed in oil-exposed seawater (Lamendella et al., 2014; Tan et al., 2015; King et al., 2015; Bruckberger et al., 2020) and compared between dispersed and non-dispersed oiled seawater (Kleindienst et al., 2015; Bera et al., 2020); however no studies to-date have investigated microbial community diversity effects between oiled seawater and ISB oiled seawater. None have investigated the factorial effects of chemical herder addition (OP-40) or under the cold-region conditions simulating the Alaska environment.

In this study, we assessed both DOM_{HC} composition and seawater microbial diversity in aquarium-scale mesocosms that contained a factorial of seawater, oil, OP-40 and ISB treatments. Such information on how chemical herder and in-situ burning affect the dissolved components of the marine environment, and thus exposure scenario to aquatic life, is relevant for informing spill response contingency plans and baseline monitoring programs. This information clarifies how each of these factors affects DOM_{HC}, what the dead-end weathered character could be, and how these conditions may affect the health of aquatic biota. This information is not well-established for Alaska and other coldregion conditions, which can be a unique exposure/toxicity scenario compared to temperate (Deepwater Horizon/Gulf of Mexico) climates. It can also be useful for future integrations of DOMHC character with toxicity assessments for other higher trophic level cold-tolerant native organisms. We hypothesized that ISB will remove most hydrocarbons compared with no treatment, will result in a higher abundance of condensed aromatic and aromatic/polyphenolic hydrocarbons compared to no treatment, and the effects magnified in herder-amended

treatments. Further, we hypothesized that microbial community diversity will differ between seawater controls, oil-only, and herded burned treatments at later time points.

2. Experimental

2.1. Chemicals and supplies

Chemicals were purchased from Fisher Scientific and VWR Scientific at ACS-grade or higher quality: acetone, 70% ethanol, hydrochloric acid, methanol, hexanes, and dichloromethane. Alaska North Slope (ANS) Crude Oil was provided gratis by Alyeska Pipeline Corporation from a blended collection at the Valdez Marine Terminal on April 4th, 2018. Siltech OP-40 herder formulation was provided by DESMI, inc. (Chesapeake, VA). TraceClean HDPE containers and Advantec GF filters (47 mm) were purchased from VWR Scientific. Aquaria (10 gallon) were previously obtained from a local pet supply store. Galvanized pans were acquired from Fastenal and storm collars from a local hardware store. Glassware and filters were pre-combusted (500 $^{\circ}C > 4$ h). All trace analysis glassware and equipment were cleaned with sequential washings of hexane, methanol, acetone, and nanopure water. HDPE sample collection carboys were soaked in 0.1 N HCl for 24 h and rinsed with DI water. Aquaria, galvanized pans, and storm collars were cleaned with Alconox and water, acetone, ethanol, and DI water rinse.

2.2. Seawater collection

Seawater was collected on April 9, 2018, near Whittier, Alaska from a near-shore site of Passage Canal, Prince William Sound on the incoming tide. Seawater hydrographic trends, for reference, are noted in Campbell (2016), including broadly for the Prince William Sound region of the Gulf of Alaska (Campbell, 2018). Collection was performed with a battery-powered peristaltic pump into 10 L acid-rinsed HDPE containers. Course particulates and zooplankton were removed using an HDPE funnel outfitted with a 200 μm mesh pre-filter. Upon collection, seawater was immediately transported to the University of Alaska Anchorage and stored at 4 °C for < 48 h prior to the start of the experiment.

2.3. Mesocosm setup

Bench-scale mesocosms of herder applications and in-situ burning were conducted similarly as described in Bullock et al. (2017). Briefly, for each sample, seawater (~3 L) was poured into a galvanized metal pan containing a centrally placed storm collar, simulating an oil release ring, leaving $\sim\!\!1$ cm of the ring exposed. Oil was dispensed into the center of the release ring and the remaining seawater was added to bring to a final volume of 5.5 L, with a surface area \sim 1297 cm². Water flowing over the release ring caused the oil to float to the top and spread out over the surface, simulating a spill. Herder additions of 0.15 mL, consistent with the recommended application rate of 50-150 mg/m² (Bullock et al., 2017) were accomplished with a micropipette around the edges of the simulated spill. The cohesive area of floating oil was ignited quickly with a butane torch, and the fire was allowed to burn until self-extinguishment. Immediately following, the entire contents of the pan were transferred into aquaria, covered with aluminum foil, and transported to the laboratory. To account for thermal degradation of microbes that may have been caused by ISB, ensuring the native microbial community consortium was present by mimicking open-water hydraulic flushing, each aquarium was brought to volume (19 L) with additional seawater and recovered. The factorial design consisted of seawater, seawater+oil, seawater+oil+ISB, seawater+oil+OP-40, and seawater+oil+OP-40+ISB. Each treatment group was created in triplicate for a total of fifteen aquaria. All aquaria were incubated in a controlled 4 °C room over 28 days.

2.4. Sample collection

Water was removed at 0-, 4-, and 28-days post-application using a dedicated, clean 1 L graduated cylinder for each aquarium, avoiding positively buoyant residues where possible. At each time point, 120 mL was collected into a TraceClean HDPE bottle for EEMs and FT-ICR MS, 900 mL into an autoclaved 1 L Nalgene bottle for DNA analysis, and 1 L into a pre-cleaned 1 L borosilicate amber bottle for TPH analysis. This resulted in a total withdrawal of 6.4 L per aquarium, or approximately 33% of the total water volume, over time. The 125 mL bottles were frozen and mailed overnight to the University of New Orleans. The 1 L Nalgene bottles were stored at $-80\,^{\circ}\mathrm{C}$ and the 1 L amber bottles were placed in a refrigerator at 4 $^{\circ}\mathrm{C}$ and extracted within 7 days of collection.

2.5. Total petroleum hydrocarbon analysis

Total petroleum hydrocarbons (TPH) of GC-amenable diesel range organics were extracted according to California Department of Fish and Game PET-PR-001 "TPH in water" (CDFG 2016). Briefly, collected water (1 L) was transferred to a separatory funnel and extracted 2x with dichloromethane (120 mL) for a total of 240 mL, with the organic phase of each extraction drained through a bed of pre-baked and solvent rinsed sodium sulfate (400 $^{\circ}$ C for 4 h) and collected into 250 mL TraceClean amber vials. Extracts were stored at −20 °C. TPH Analysis was performed using an Agilent 7890 A Gas Chromatograph Flame Ionization Detector (GC-FID) equipped with a split/splitless injector (250 °C), a flame ionization detector (350 °C), and an Agilent J&W HP-5MS capillary column 30 m x 0.25 mm i.d. x 0.25 µm film thickness. Sample volume of 1 µL was auto-injected with an oven temperature program set to hold at 50 °C for 2 min then increase to 325 °C at a rate of 15 °C/min then hold at 325 °C for 20 min, resulting in a total run time of 40.3 min. Concentrations for individual alkanes C10-C36 were reported using internal standard ortho-terphenyl. Total hydrocarbon content was determined through summation of all peak areas, excluding the peak areas for the solvent and internal standards. Analyte concentrations were determined relative to the internal standard concentration, using calibration equations obtained from 5-point calibration curves created using serial dilutions of Restek ASTM Method D2887 calibration standards. An experimental blank (DCM), reference standard, and an untreated dilute oil sample were included in all test batches. Short-chain (C10 - C18) and long-chain (C20 - 36) alkanes removal percentages were calculated by:

$$\% \ removal = (1 - C_i/C_o) \times 100\%$$

where C_i is the sum of the analyte concentrations for the short- (or longchain) alkanes at each experimental time point for each treatment and C_0 is the sum of the analyte concentrations for the short- (or long-chain) alkanes for seawater with oil on day 0 (Olson et al., 2017; Lin and Mendelssohn, 2009).

2.6. Dissolved organic carbon

Thawed water samples were filtered through pre-combusted ($450\,^{\circ}\mathrm{C} > 4\,\mathrm{h}$) Advantec GF 0.3 µm glass fiber-filter into a precombusted ($500\,^{\circ}\mathrm{C} > 4\,\mathrm{h}$) amber glass vial. The pH of each sample was immediately adjusted with ultrahigh purity hydrochloric acid to pH < 2 and samples stored in the dark at 4 °C until DOC analysis. Nonpurgeable dissolved organic carbon was measured by high temperature combustion with a Shimadzu TOC Vcsn analyzer. The sample concentrations were determined using a five-point calibration curve between 0 and 50 ppm of potassium hydrogen phthalate (KHP). Blank injections were run in between each sample injection, and bracketing standards were run every 10 sample injections and at the end of the analyses. To ensure the samples were within the calibration curve, the auto dilution feature on the TOC analyzer was enabled. Acidified samples were sparged for 5.5 min at 75 mL/min with ultrapure air to

remove inorganic carbon from samples prior to the measurement. Reported DOC concentrations are the means of three to six replicate injections of 50 μ L for which the coefficient of variance was <2%.

2.7. Optical analyses

Filtrate splits from the DOC samples (described above) were adjusted to pH 6-8 for absorbance and fluorescence measurements using an Aqualog® fluorometer (Horiba Scientific, Kyoto, Japan) (Spencer et al., 2007; Tfaily et al., 2011; Yan et al., 2013). Measurements were completed in a 10 mm quartz cuvette at a constant temperature of 20 $^{\circ}$ C. Absorbance and excitation scans were collected from 240 to 800 nm in 5 nm increments with an integration period of 0.5 s. Milli-Q water $(18.2~\text{M}\Omega~\text{cm}^\text{-1})$ was used to dilute each sample to an absorbance of 0.1at 254 nm to reduce inner filter effects when necessary (Ohno, 2002; Kowalczuk et al., 2003). Spectra were blank subtracted and corrected for instrument bias in excitation and emission prior to correction for inner filter effects. Fluorescence intensities were normalized to Raman scattering units prior to Parallel Factor (PARAFAC) statistical analysis. PARAFAC analysis of excitation-emission matrix spectra (EEMs) obtained for the water samples was applied using drEEM toolbox v. 5.0 (tutorial and MatLab code) (Murphy et al., 2013). The spectral properties for each of the components were examined and then validated by residual and split-half analysis (Harshman, 1984; Stedmon and Bro, 2008). The components from this PARAFAC model were matched to others reported in the OpenFluor database that have a Tucker's congruence coefficient threshold of 0.95 for an identical match between spectra (Murphy et al., 2014). The humification index (HIX) was calculated by dividing the area under an emission range of 435-480 nm by the sum of the peak area of 300-435 and 435-480 nm, with excitation at 254 nm (Ohno et al., 2007). Freshness Index (FRESH) was calculated at excitation 310 nm and the intensity of 380 nm divided by the maximum emission between 420 and 435 nm (Parlanti et al., 2000; Williams et al., 2010). Other optical proxies were calculated to assess changes in aromaticity, size, and reactivity of DOM_{HC} (Ohno et al., 2007; Hansen et al., 2016; Fellman et al., 2010; McKnight et al., 2001).

2.8. Fourier transform ion cyclotron mass spectrometry

Filtrate splits from DOC collections were pre-concentrated by the solid-phase extraction technique described by Dittmar et al. (Dittmar et al., 2008). Briefly, each sample was passed through a pre-combusted 0.3 µm glass-fiber filter at pH 2 prior to loading onto a Bond Elut PPL (Agilent Technologies) stationary phase cartridge. Each sample was desalted with pH 2 Milli-Q water and eluted with methanol at a final concentration of 50 µgC mL⁻¹. The extraction efficiency of petroleum-derived DOM by PPL across a compositional gradient is reported elsewhere by Zito et al. (Zito et al., 2019a). The extracts were stored in the dark at 4 °C in pre-combusted glass vials until analysis by negative-ion electrospray ionization (ESI) coupled with a custom-built Fourier transform ion cyclotron resonance mass spectrometer (FT-ICR MS) equipped with a 21 tesla superconducting magnet at the National High Magnetic Field Laboratory (NHMFL), Florida State University, Tallahassee (Smith et al., 2018). Each mass spectrum was internally calibrated with a "walking" calibration equation (Savory et al., 2011) followed by molecular formula assignment with EnviroOrg software provided by the NHMFL (Corilo, 2015; Savory et al., 2011). Molecular formulae were classified based on stoichiometry into condensed aromatic (CA) (modified aromaticity index (AI $_{mod} \geq 0.67$), aromatic (0.67 > AI_{mod} > 0.5), unsaturated, low oxygen (ULO) (AI_{mod} < 0.5, H/C < 1.5, O/C < 0.5), unsaturated, high oxygen (UHO) (AI $_{mod}$ < 0.5, H/C <1.5, O/C \geq 0.5), and aliphatic (H/C \geq 1.5)(O'Donnell et al., 2016; Koch and Dittmar, 2006; Santl-Temkiv et al., 2013). Abundance weighted molecular weight (MWw), nominal oxidation state of carbon (NOSCw), O/C, and H/Cw were also calculated from the MS data (Riedel et al., 2012; Spencer et al., 2019; He et al., 2020). Reproducibility of data

acquired by ESI ultrahigh resolution mass spectra for individual samples on multiple different instrument platforms is reported in detail by Hawkes et al. (2020) (Hawkes et al., 2020).

2.9. Microbial community analyses

2.9.1. DNA extraction and sequencing

Water reserved for Deoxyribonucleic acid (DNA) extraction (900 mL) was filtered using 0.22 µm PES membrane filters (47 mm round; Millipore Express Plus membrane filters) and filters were stored at $-80\,^{\circ}\text{C}$ until extracted. DNA was extracted from filters as described by Boström et al. (Boström et al., 2004). Briefly, half of a filter was cut into small pieces and placed into a 15 mL conical tube with 2 mL lysis buffer (400 mM NaCl, 750 mM sucrose, 20 mM EDTA, 50 mM Tris-HCl adjusted to pH 8.3 with NaOH) and 200 µL lysozyme (1 mg/mL, final concentration), incubated at 37 °C for 30 min, followed by an overnight incubation at 55 $^{\circ}C$ with 225 μL 10% SDS and 20 μL proteinase K (100 mg/mL). The filtered samples were held at temperature in an orbital shaker during incubation. DNA was precipitated with 0.1 vol of 3 M sodium acetate and 0.6 vol isopropanol for 1 h at -20 °C. Samples were centrifuged at 13,000 g for 20 min and the supernatant was discarded. The remaining pellet was washed with 80% and then 100% ethanol, air dried and resuspended in Tris EDTA (TE; 1x). DNA concentration and purity were measured with a Qubit fluorometer (Invitrogen; Carlsbad, California, USA) and extractions were held at -80 °C until amplified and sequenced.

The V4 region of the 16 S rRNA gene was PCR-amplified in triplicate using universal bacterial primers 515F (5'-3')GTGCCAGCMGCCGCGGTAA with Illumina adapter AATGA-TACGGCGACCACCGAGATCTACAC, primer pad CGTGGTGGTC and forward primer linker GT) (Caporaso et al., 2012) and 806R (5'-3' CAAGCAGAAGACGCCATACGAGAT and 8-bp Golay barcode with illumina adapter CAAGCAGAAGACGGCATACGAGAT, primer pad AGT-CAGTCAG and primer linker CC) (Bolyen et al., 2019) according to the Earth Microbiome Project protocol (available in the public domain at www.earthmicrobiome.org) (Gilbert et al., 2010). Sample amplifications were pooled in triplicate and purified using AxyPrep Mag PCR clean-up (Axygen; Union City, California, USA). Amplicons were combined in equimolar amounts and final library concentration was determined using Kapa Library Quantification Kit (Roche Sequencing Solutions Inc., Pleasanton, CA). At all PCR steps, amplification success and purity were checked by gel electrophoresis. Paired-end sequences $(300 \times 2 \text{ bp})$ were generated from barcoded amplicon products using Illumina MiSeq platform (MiSeq v2 Reagent Kit). All raw 16 S rRNA gene sequences have been submitted to the DDBJ/EMBL/GenBank databases under accession numbers SRR12486038-12486083.

2.9.2. Sequence analyses

Illumina sequencing data were processed with QIIME2 (v.2019.1) (Bolyen et al., 2019). Briefly, sequences were demultiplexed and quality filtered using QIIME 2 (q2)-demux emp-paired plugin followed by joining using q2-vsearch join-pairs. Joined sequences were then quality filtered using q-score-joined and denoised using q2-deblur (Amir et al., 2017) to identify all observed amplicon sequence variants (ASVs). Samples were filtered to remove ASVs that were represented less than 5 times. Remaining ASVs were aligned using MAFFT (Katoh and Standley, 2013) and used to construct a phylogeny with FasTtree2 (Price et al., 2010). Taxonomy was assigned to ASVs in QIIME2 using the Naive Bayes classifier and q2-feature-classify-sklearn plugin (Bokulich et al., 2018) against Greengenes 13_8 99% OTUs reference sequences (McDonald et al., 2012).

2.9.3. Statistical analysis

Samples were rarefied to a depth of 999 sequences prior to alpha diversity analysis, to minimize sample loss from the dataset. Three alpha diversity metrics were calculated: number of observed ASVs, Shannon's

H (Shannon, 1948), and Faith's Phylogenetic Diversity (PD) (Faith, 1992). Statistical differences between treatments and sampling days were determined for all three metrics using ANOVAs, and pairwise differences within variables were calculated using TukeyHSD tests with a bonferroni correction for multiple comparisons (Dunn, 1961).

Microbiome community composition was analyzed using the phyloseg package (v. 3.2.1) (McMurdie and Holmes, 2013) and results were visualized using the ggplot2 package (Wickham, 2016) in R (Wickham and Sievert, 2016). Non-metric multidimensional scaling (NMDS) analysis was applied to three distance matrices: Bray-Curtis (Bray and Curtis, 1957) unweighted UniFrac and weighted UniFrac distances (Lozupone and Knight, 2005). Beta dispersion of the Bray-Curtis distance was calculated for sampling day and treatment using the betadisper function, and statistically compared among treatments and days using the permutest function from the vegan package (v. 2.5.6) (Oksanen et al., 2019). To determine whether sampling day and treatment were correlated with microbiome composition, permutational multivariate analysis of variance (perMANOVA) was used with the adonis function from the vegan package. In addition, the pairwise perMANOVA function from the RVAidememoire package (v.0.9-77) was used to identify which treatment and sampling day differences drove possible statistically significant results (Hervé, 2018).

Bacterial abundances were summarized at phylum and genus levels and bar plots of relative abundance were generated for all phyla, and genera within Proteobacteria. Genera that represented less than one percent of the total relative abundance were excluded for clarity from taxonomic bar plots and charts.

Differential abundance of genera in different treatments compared to the Seawater control was determined using the *DeSeq2* package (v. 1.24.0) in R (Love et al., 2014). *P*-values were corrected with the Benjamini and Hochberg false discovery rate for multiple testing (Benjamini and Hochberg, 1995). Genera were identified as differentially abundant if the corrected p values < 0.05.

3. Results and discussion

3.1. ISB observations

When crude oil was ignited in bench-scale pans, a typical burn persisted for approximately 1.5 min and resulted in an increasing water temperature by 2 °C (5.5 L volume). Addition of OP-40 prior to ignition successfully collected oil at the center of the pan, burned longer (approximately 2 min), increased the water temperature by 7 °C, and resulted in visually less burn residue mass. While the vast majority of burn residue was effectively transferred to each aquarium, a small amount of viscous residue remained on the aluminum pan. Once transferred to aquaria and diluted to 19 L, a combination of positive, negative, and neutrally buoyant residues remained in suspension throughout the incubation period, consistent with prior observations of high molecular weight tar-like burn residue (Fingas, 2018; Stout and Payne, 2016), which were not removed throughout the time course of the experiment. A slight odor originating from volatiles of non-combusted ANS crude oil, occurred initially but decreased significantly after day 0.

Bullock et al. demonstrated that bench-scale burns using this identical approach achieve $\sim 40\%$ reduction in oil mass, while larger "meso scale" (3 m x 3 m) burns attain up to $\sim 70\%$, and field scale may approach 80% (Bullock et al., 2017). This study indicated scale-up considerations since combustion efficiency increases with intensity. In this study, operation on the bench-scale was selected to allow a more controlled environment and higher replication for the same logistical effort. These findings are conceptual in nature and are not intended to be a direct comparison to larger-scale burns; those conducted on the smaller scale like the ones in this experiment tend to produce a less complete combustion (Bullock et al., 2017, 2019). Despite our experiment operating on a smaller scale, the conceptual trends from these

burns may provide some insight into water-soluble residues that may occur from this process. In future studies, scalability of these findings will be assessed. Following combustion, positively buoyant residues were apparent (which in a spill scenario may be destined for mechanical surface recovery), while negatively buoyant residues were observed as well. Due to the heterogeneity of this distribution, no post-burn residue was removed and therefore, the estimates of the dissolved fraction may represent a conservative "worst-case" scenario and are understood that an open-ocean surface burn would exhibit unique characteristics.

3.2. Total petroleum hydrocarbons

The average recovery for 5-alpha androstane was $100 \pm 10\%$ for seawater treated with oil, $104 \pm 10\%$ for seawater treated with oil and ISB, 118 \pm 12% for seawater treated with oil and OP-40, and 89 \pm 13% for seawater treated with oil, OP-40, and ISB. All of which fall within the 70-120% EPA criteria (USEPA, 2016; Turner et al., 2014). The total alkane concentrations (Fig. 1A) decreased for all oil-treated samples over the course of the 28-day experiment. On day 28, burned samples revealed significant deviations from non-burned (p < 0.05). These Σn -alkane data revealed comparable concentrations between ISB+OP-40 and SW controls, indicating a high efficiency removal of n-alkanes. Σn -alkane concentrations between seawater controls and herded burned samples were not significantly different post initial treatment on day 0. Given that dichloromethane extraction is selective for non-polar analytes and GC-FID analysis is selective for boiling point ranges < 320 $^{\rm o}$ C, ISB removed the analytes observed in this analytical window. Comparison of percent removal of short-chain (C10 - C18) versus long-chain (C20 - 36) alkanes (Fig. 1B/C) indicates a preferential removal/degradation of short-chain alkanes. No significant temporal changes in the concentration of short- or long- chain alkane removal was observed for herded burned samples; removal percentages at the end of the experiment reached 98% and 96%, respectively by day 28. The alkane removal percentages for short- and long- chain alkanes in seawater treated with oil and not remediated peaked at 93% and 80%, respectively; significantly higher than the removal percentages observed for samples remediated with herder; indicating OP-40 may have hindered the natural, microbial degradation processes.

3.3. Dissolved organic carbon

DOC measurements represent a total mass of petroleum-derived C when subtracted from seawater controls sampled at the same time point. This includes both GC-amenable, non-purgeable dissolved organic carbon and non-volatile fractions. The mean seawater+oil DOC concentrations at day 0 were higher compared to seawater alone (Fig. 2), 17.7 mg/L vs. 5.4 mg/L. As each aquaria aged, DOC degraded with time,

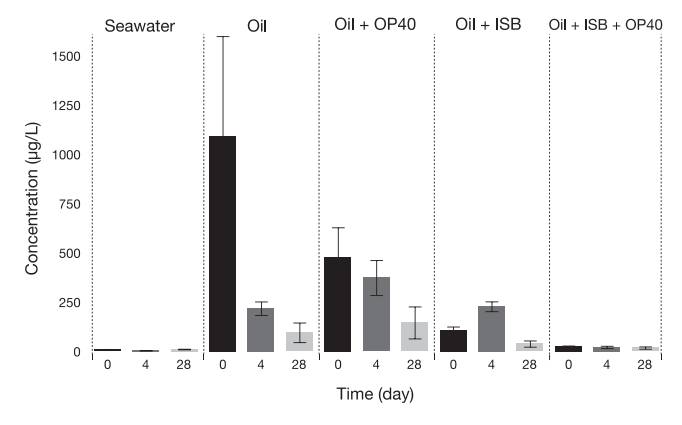


Fig. 1. Concentration of total alkanes (C10 – C44) for seawater, oil, oil + OP40, oil + ISB, and oil + ISB + OP40. Samples collected on day 0 (black bars), 4 (dark grey) and 28 (light grey). $N=3\pm SE$.

down to 2.3 and 1.4 mg/L, respectively, at day 28. When herder was applied to oil but not combusted, a similar day 0 trend was evident, where oil+OP-40+seawater was elevated compared to seawater by 8.3 mg/L. However, over time, a higher concentration of DOC was observed in SW+oil+OP-40 after day 28 compared to SW +oil alone, 8.6 vs. 2.3 mg/L, respectively. When SW+oil was burned, both herded and unherded samples were significantly lower in DOC at day 0 (4.8 and 2.1 mg/L, respectively). However, as these aquaria aged, both herded and unherded samples expressed an increase in DOC at day 4–11.5 and 10.9 mg/L, then decreased between two levels of 4.8 and 4.5 mg/L at day 28. This behavior is consistent with slow dissolution of burned residues, which degrade slowly and remain elevated compared to seawater DOC at day 28. The SW+oil+OP-40+ISB and SW+oil+ISB did not express significant differences between DOC concentrations at any time point (student's t-test, 95% confidence).

3.4. Optical spectroscopy

3.4.1. Spectral features

A five component PARAFAC model was validated and is provided in Fig. 2, Figure S1, and Table S1. Previous studies applying PARAFAC statistical analysis to EEMs to characterize the petroleum-derived DOM signatures have been widely reported in both marine and freshwater ecosystems (Zito et al., 2019b; Podgorski et al., 2018, 2021; Bianchi et al., 2014; Ray et al., 2014; Zhou and Guo, 2012; Bugden et al., 2008; Harriman et al., 2017; Dvorski et al., 2016). Component 1 (C1) is shifted to a longer emission wavelength than C3 with excitation maximum at < 250 nm and emission maximum at 360 nm. A component with similar spectral properties was identified in samples collected from the Amazon River Basin and was shown to be correlated with relatively low molecular weight (MW), aromatic, oxidized compounds (Gonsior et al., 2016). C1 also matches components associated with DOM derived from thermogenic sources in the OpenFluor database. One of the matches was with a component that was associated with thermogenic DOM in sediment porewater and the overlying water column produced from a mud volcano in the Beaufort Sea (Retelletti Brogi et al., 2019). The other match is with a component that is characterized as a biorefractory component in a groundwater plume originating from an oil body at the National Crude Oil Spill Fate and Natural Attenuation Research Site near Bemidji, MN, USA (Podgorski et al., 2018, 2021). Murphy et al. (2013) showed the presence of an unidentified component (C4) in their PAR-AFAC model with Ex/Em similar to pyrene from ship ballast water suggesting the presence of PAHs in their marine samples (Murphy et al., 2006). The unidentified C4 component in the Murphy et al. (2013) study had an Ex/Em maxima of 250/370 nm matching C1 from the model validated in the current study (Fig. S1). C1 had the highest variation explained for all the components which decreased from C1 to C5 (Fig. 2) (Fellman et al., 2010; Murphy et al., 2006). The presence of "peak-U" from Murphy et al. (2013) and its presence in this study generated from petroleum in a controlled environment, provides further evidence of its identity as a PAH signature.

PARAFAC Component 2 (C2) is the component with the shortest emission reported in this study. This component has excitation maximum at 270 nm and emission maximum at 308 nm which is commonly referenced as "tyrosine-like" fluorescence which was observed as the most prominent peak in Fig. 2, Fig. S1, and Table S1 (Yamashita et al., 2013, 2011; D'Andrilli et al., 2019). Component 3 (C3) is shifted to slightly longer Ex/Em wavelength than C2 with excitation maximum at 285 nm and emission maximum at 337 nm. Fluorescence in this wavelength region is commonly called "tryptophan-like". Collectively, C2 and C3 comprise fluorescence signals associated with "protein-like" signatures (Lapierre and del Giorgio, 2014; Cory and McKnight, 2005; Kothawala et al., 2014). Petroleum derived compounds with fluorescence in the C2 and C3 regions are associated with relatively reduced, aliphatic DOM. However, in addition to matching "tyrosine-like" components in the OpenFluor database, C3

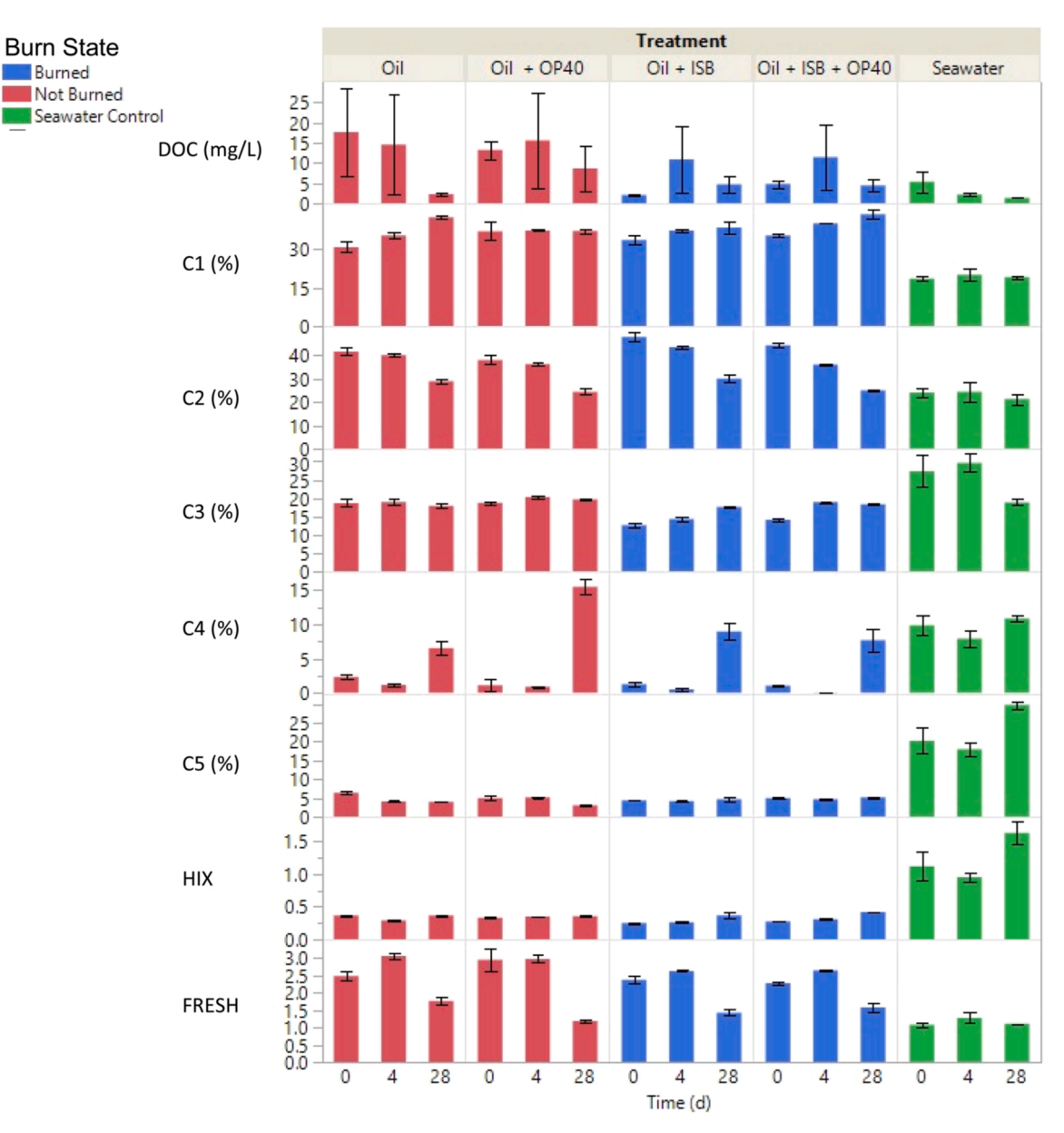


Fig. 2. Dissolved organic carbon concentration, relative contribution of PARAFAC components C1-C5, humification index (HIX), and freshness index (FRESH) in the dissolved fractions of oil, oil with herder, and oil that was burned with and without herder.

also exhibits spectral properties like dissolved polycyclic aromatic hydrocarbons (PAHs) in ballast and other petroleum contaminated waters (Murphy et al., 2006; Mirnaghi et al., 2019). The spectrum for component 4 (C4), with excitation maximum at 300 nm and emission maximum at 408 nm is like classical "peak-M" that is associated with low MW marine humic material (Kowalczuk et al., 2013; Coble, 1996). Finally, C5 is known as the "peak-A, C", "humic-/fulvic-like" fluorescence. This component matches those in the database associated with high MW, aromatic, highly oxidized compounds derived from terrestrial sources (Gonçalves-Araujo et al., 2016; Tomco et al., 2019).

3.4.2. Optical trends in composition

Fig. 2 and Table S1 show the relative contribution of each PARAFAC component for all water samples and time points from oil, oil+OP-40, oil+ISB, Oil+ISB+OP-40, and the seawater control. C1 has the second highest contribution in all of the samples that were in contact with oil. The contribution of C1 is $30.9\pm3.4\%$ for the oil sample, $33.7\pm3.1\%$ for ISB, and $35.4\pm1.1\%$ in the ISB+OP40 sample (Fig. 2, Table S1). The relative values of C1 for the water samples that were in contact with oil

are nearly double that of C1 in seawater (18.5 \pm 1.6%) (Table S1). This result is indicative of dissolution of petroleum compounds. The oil (35.5 \pm 2.4%, 42.6 \pm 0.7%), oil+ISB (37.4 \pm 1.0%, 38.6 \pm 4.1%), and oil+ISB+OP40 (40.2 \pm 0.2%, 43.7 \pm 2.9%) each show a relative increase in the percent contribution of C1 and no change for Oil+OP40 (37.4 \pm 0.6, 37.2 \pm 1.4) after 4 and 28 days of incubation, respectively. An increase or in the contribution of C1 along with a subsequent decrease in DOC concentration is an indicator that the components associated with C1 persist. The result is consistent with the detection of microbially refractory compounds derived from petroleum in other aquatic ecosystems (Podgorski et al., 2021; Han et al., 2008).

The relative contribution of C2 is highest for samples that were in contact with oil (41.6 \pm 2.8%), oil+ISB (47.9 \pm 3.5%), oil+OP40 (38.0 \pm 3.4) and oil+ISB+OP40 (44.5 \pm 1.2%) at day 0 (Fig. 2, Table S1). The contribution of C2 in each of these samples is nearly twice the contribution of C2 in the native seawater (24.0 \pm 3.0%). Although fluorescence like C2 is commonly referred to a "tryptophan-like", the increase in the relative contribution of C2 compared with the seawater is likely due to dissolution of relatively low molecular weight, aliphatic

hydrocarbons that fluoresce in this region (Podgorski et al., 2018, 2021). The contribution of C2 in the burned samples is slightly higher than the oil alone. This result may be due to thermal degradation of hydrocarbons into small aromatics with relatively low fluorescence excitation/e-mission maxima (Retelletti Brogi et al., 2019). Unlike C1, the percent contribution of C2 decreases in all treatments, oil (40.2 \pm 1.4%, 28.9 \pm 1.7%), oil+ISB (43.6 \pm 1.4%, 30.1 \pm 2.9%), oil+OP40 (36.3 \pm 0.8%, 24.5 \pm 2.0%), and oil+ISB+OP-40 (36.1 \pm 0.3%, 25.0 \pm 0.7%) after 4 and 28 days of microbial incubation, respectively. This result indicates that the compounds associated with C2 are labile, matching previous reports in the literature (Podgorski et al., 2018; Yamashita and Tanoue, 2003; Davis and Benner, 2007).

Component 3 exhibits two different trends that are associated with the presence or absence of ISB. The highest C3 values are measured in the oil (18.9 \pm 1.3%) and oil+OP40 (18.8 \pm 0.8) at day 0 (Fig. 2, Table S1). The values for C3 remain relatively constant in the unburned samples, oil (19.0 \pm 1.2%, 19.9 \pm 0.9%), oil+OP40 (20.3 \pm 0.9%, $19.7 \pm 0.2\%$) after 4 and 28 days of incubation, respectively). The percent contribution of C3 at day 0 are lower for the oil+ISB (12.7 \pm 0.9%) and oil+ISB+OP40 (17.6 \pm 0.6%) compared with their unburned analogues. Both of the burned treatments showed an increase in C3 after incubation. The percent contribution of C3 increased to $14.3 \pm 0.9\%/17.6 \pm 0.6\%$ in the oil+ISB and $19.0 \pm 0.4\%/18.4 \pm 0.6\%$ after 4 and 28 days of incubation. This result is likely due to the formation of relatively small, aromatic, oxidized, black carbon-like compounds that are water-soluble. These types of compounds are resistant to microbial degradation. The result is a relative increase in the contribution of this fluorescence component as these compounds persist while others degrade (Podgorski et al., 2021).

The trends in percent contribution of C4 are similar across all treatments. The initial (Day 0) contribution of C4 are $2.3 \pm 0.5\%$, $1.3\pm0.5\%$, $1.1\pm1.4\%$, and $1.0\pm0.1\%$ for the oil, oil+ISB, oil+OP40, and oil+ISB+OP40, respectively (Fig. 2, Table S1). A relative decrease in C4 after 4 days of microbial incubation is observed for the oil (1.2 \pm 0.4%), oil+ISB (0.5 \pm 0.3%), oil+OP40 (0.9 \pm 0.1%), and oil-+ISB+OP40 (0.1 \pm 0.0%). The decrease in the percent contribution of C4 in each treatment after 4 days of microbial incubation is an indication that the initial composition of compounds in this fluorescence region are (semi-) labile. Conversely, the percent contribution of C4 increases substantially for each treatment after 28 days of incubation, oil (6.54 \pm 1.84%), oil+ISB (9.0 \pm 2.2%), oil+OP40 (15.5% \pm 2.0%), and oil+ISB+OP40 (7.7 \pm 2.8%). This result is likely due to the formation of relatively small, aromatic, oxidized, degradation products. Unlike the compounds that fluoresce in this region at Day 0, these "dead-end" products are not microbially labile and persist in the water samples.

The trends in the percent contribution of C5 are related to the presence or absence of burning (Fig. 2, Table S1). The contribution of C5 for the oil and oil+OP40 are 6.5 \pm 0.6% and 5.0 \pm 0.2% respectively. After 4 and 28 days of incubation, the relative contribution of C5 decrease in both unburned oil (4.1 \pm 0.3%, 4.0 \pm 0.1%) and oil+OP40 $(5.2 \pm 0.2\%, 3.1 \pm 0.3)$ treatments. These trends are likely due to petroleum dissolution processes that contribute relatively aliphatic compounds that overprint fluorescence in the C5 region that is more closely associated with carboxyl-rich alicyclic molecules (CRAM) that are found in marine waters (Hertkorn et al., 2006). Different trends are observed for the burned samples. The percent contribution of C5 is relatively constant for the oil+ISB and oil+ISB+OP40 treatments. The contribution at day 0 in the oil+ISB is 4.4 \pm 0.2%, 4.2 \pm 0.2% after 4 days of incubation, and 4.7 \pm 1.1% after 28 days. Similarly for oil+ISB+OP40, the percent contribution of C5 is 5.0 \pm 0.2% at day 0, 4.7 \pm 0.4 after 4 days, and 5.2 \pm 0.3% after 28 days of microbial degradation. The relative stability of C5 in the burned samples may indicate that highly oxidized, CRAM-like compounds are formed after ISB. Moreover, the result may be due to persistent signatures of CRAM-like compounds in the marine water.

The HIX indices (Fig. 2, Table S1) decrease after each treatment

when compared to the seawater control. This result is due to the dissolution of relatively aliphatic compounds that occurs when the oil encounters the water. The seawater control HIX value increased after 28 days of microbial processing illustrating a depletion of (semi-) labile compounds and enrichment of refractory of CRAM-like compounds. The trends in HIX values are closely associated with their burn state. The HIX values for unburned oil are $(0.37 \pm 0.0, 0.29 \pm 0.0, 0.37 \pm 0.0)$ and oil+OP40 (3.3 \pm 0.0, 3.5 \pm 0.0, 3.6 \pm 0.0) after 0, 4, and 28 days of incubation. The decrease in HIX in the oil sample after 4 days of incubation may be related to a pulse of fresh labile DOM_{HC} that is a result of dissolution processes. Although the trend in HIX for the oil+OP40 on increases slightly as a function of incubation time, the result indicates that the composition of the mixture is becoming more aromatic and oxygenated. More pronounced trends are observed in the burned treatment. The initial (day 0) HIX values for the oil+ISB and oil-+ISB+OP40 are 0.25 \pm 0.0 and 0.27 \pm 0.0. These values are smaller than their unburned counterparts indicating that these mixtures are composed of relatively reduced compounds. Both the oil+ISB $(0.26 \pm 0.0, \ 0.37 \pm 0.1)$ and oil+ISB+OP40 $(0.31 \pm 0.0, \ 0.42 \pm 0.0)$ exhibited marked increases in HIX values after 4 and 28 days of incubation that surpass those of the unburned samples. This result is like due to the formation of both relatively aliphatic, reduced and aromatic, oxygenated compounds (and/or CRAM) that are microbially refractory.

The freshness index (FRESH) for all treatments was higher than the seawater controls and decreased after 28 days of biodegradation. The most notable feature in the trends for FRESH is the increase after 4 days of incubation prior to the decrease after 28 days. The day 0 FRESH values for the oil, oil+ISB, oil+OP40, and oil+ISB+OP40 are 2.5 ± 0.2 , 2.4 ± 0.2 , 3.0 ± 0.6 , and 2.3 ± 0.0 respectively. After 4 days of incubation, the FRESH values for each treatment increase to oil (3.1 \pm 0.2), oil+ISB (2.6 \pm 0.0), oil+OP40 (3.0 \pm 0.2), and oil+ISB+OP40 (2.7 \pm 0.0) when compared to their respective day 0 treatment. The increase in these values after 4 days of treatment is indicative of a pulse of labile DOM_{HC} that is entering the systems. This pulse is likely associated with dissolution of labile petroleum compounds. There is a marked decrease in FRESH values for oil (1.8 \pm 0.2), oil+ISB (1.4 ± 0.2) , oil+OP40 (1.2 ± 0.1) , oil+ISB+OP40 (1.6 ± 0.2) after 28 days of microbial incubation. The stark decrease of FRESH values after 28 days of incubation indicates that (semi-) labile petroleum compounds from both unburned and burned treatments are degraded by microbes.

3.5. Fourier transform ion cyclotron resonance mass spectrometry

Ultrahigh resolution mass spectrometry is a useful technique for determining the molecular-level composition of complex mixtures. Although this technique may provide a wealth of information, there are limitations that result from ion efficiency of analytes. In our experiments, we used natural seawater that contained DOM. The DOM components in our seawater ionized efficiently and at times, overprinted the signal from our analytes of interest produced from the petroleum source. We used several different data reduction strategies to extract information from these data sets. It is important to note that these results may only be interpreted qualitatively.

3.5.1. Molecular diversity

Fig. 3 and Table S2 show the number of assigned molecular formulae and % relative abundance of the compositional classes as determined by FT-ICR MS. On average, the ISB treatment samples had more assigned formulae at any given incubation time point. As a function of incubation time, the average number of molecular formulae slightly increases for the unburned oil and oil+OP40 after 28 days of incubation (Fig. 3 and Table S2). Conversely, there is a slight decrease in the average number of molecular formulae associated with the ISB samples after 28 days of incubation. These trends are likely a result of the production of a broad spectrum of oxygen-containing molecular formulae in the samples after ISB (Figs. 2, 3, and S1, Tables S1 and S2). The oil and oil+OP40 samples

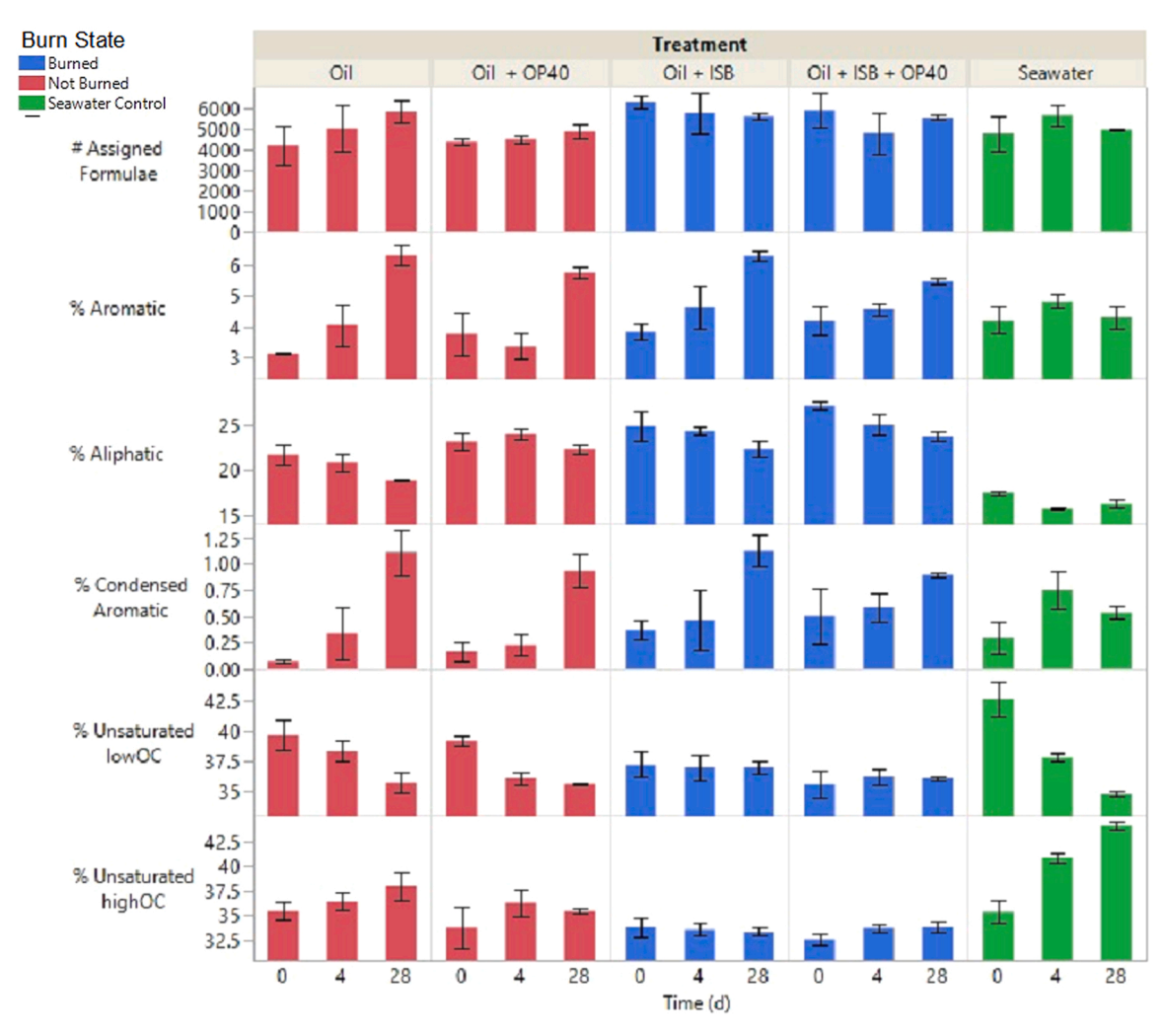


Fig. 3. Number of assigned molecular formulae and the percent relative abundance (%RA) of the aromatic, aliphatic, condensed aromatic, unsaturated low oxygen, and unsaturated high oxygen classes.

have a limited number of water-soluble compounds. As these water-soluble compounds are microbially degraded, there is an increase in molecular diversity due to the formation of oxygen-containing degradation products (i.e., increase in the number of molecular formulae). On the other hand, the molecular diversity of the products produced from ISB is slightly reduced by microbial degradation processes. This result may be due to complete mineralization of some labile oxygen-containing aliphatics that are produced from ISB.

3.5.2. Molecular-level composition

Compositional trends between each treatment are shown in Fig. 3 and Table S2. As expected, there is an increase in the average %RA of both the aromatic and condensed aromatic classes in both the oil and oil+herder increased after ISB. As observed in the subtraction subplots shown in Fig. 4, there is an enrichment of the average %RA of the aromatic and condensed aromatic classes after 28 days of incubation. For both the herded and non-herded samples, there is an increase in the % RA of aliphatic compounds after ISB due to the production of watersoluble incomplete combustion products from the aliphatic crude oil. As a function of incubation time, each treatment exhibits a decrease in the average %RA of the aliphatic compounds. This result is consistent with selective microbial degradation of aliphatic compounds. Moreover, the observed decrease in the aliphatics by FT-ICR MS mirrors trends in the labile fraction of the DOM_{HC} that can be measured by optical spectroscopy (C2, FRESH). The average %RA of the saturated low oxygen class is initially highest in the oil and oil+herder treatments prior to ISB.

There is a decrease in the %RA of this class following ISB. Notably, there is a decrease in the %RA of this class as a function of incubation time for the samples that were not burned. Conversely, the %RA of the unsaturated low oxygen class remains relatively consistent in both the oil and oil+herder treatments after ISB. This result is indicative of the continuum of compounds within this classification where those that are relatively more saturated are likely more microbially labile than the relatively unsaturated compounds within the same class. Finally, there is an observed decrease in the unsaturated high oxygen in the samples following ISB relative to the unburned samples. This result may be attributed to overprinting of the DOM_{HC} with the natural background marine DOM in our water samples. Nevertheless, we contend that the ISB process produces DOM_{HC} compounds with a higher degree of oxygenation relative to the unburned samples (Jaggi et al., 2019).

Molecular formulae classified as aliphatic (H/C \geq 1.5) are known to be microbially labile (Spencer et al., 2019, 2014; Podgorski et al., 2021; D'Andrilli et al., 2015; Goranov et al., 2021). There is a high abundance of oxygen-containing aliphatic compounds produced in both the oil and oil+OP40 after in-situ burning (Fig. 4a-d). A large fraction of those compounds is degraded by microbial processes after 28 days of incubation. There are 1954 DOM_{HC} molecular formulae that are "removed" and 753 "produced' from the in-situ burned oil after 28 days of incubation (Fig. 4f-g). A similar trend is observed for the in-situ burned oil+OP40 after incubation, where 1801 formulae are removed and 886 are produced (Fig. 4h-i). In both treatments, aliphatics are selectively removed and aromatic compounds are preserved. These results are

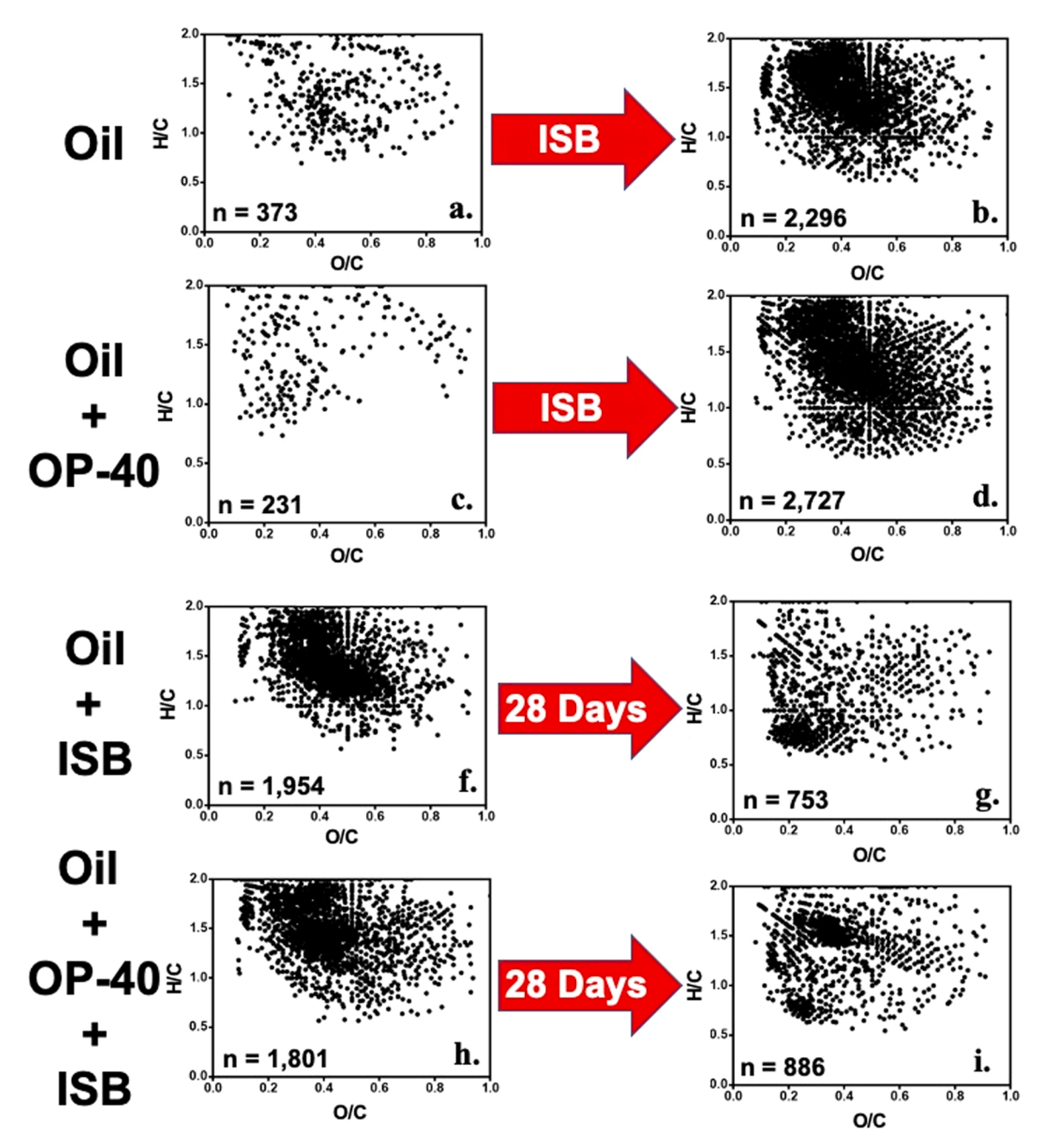


Fig. 4. van Krevelen diagrams of unique DOM_{HC} molecular formulae to oil before (a) and after (b) in-situ burning, oil and herder before (c) and after (d) in-situ burning, in-situ burned oil at day 0 (f) and after 28 days of microbial degradation (g), and in-situ burned oil with herder at day 0 (h) and after 28 days of microbial degradation (i).

consistent with previous reports on the microbial lability of DOM_{HC} (Harriman et al., 2017; Podgorski et al., 2021). Moreover, the results obtained by FT-ICR MS corroborate those obtained by quantitative DOC measurements and complementary optical spectroscopy (Fig. 2). The "removal" of formulae after 28 days of incubation is corroborated by a decrease in DOC concentration. Moreover, selective removal of relatively aliphatic compounds and conservation of relative aromatic compounds observed by FT-ICR MS after 28 days of incubation is corroborated by the decrease in C2 and FRESH and a corresponding increase in HIX.

van Krevelen subtraction plots of select samples (Fig. 4) highlight the trends observed in Fig. 3. There are changes in the chemical composition as a function of both treatment and time. The most notable changes in the molecular-level composition of DOM $_{\rm HC}$ between treatments are before and after in-situ burning. Fig. 4a-d shows van Krevelen diagrams

of formulas that are unique to oil, oil+OP40, and oil+ISB+OP40 at day 0. There is approximately a six-fold increase in the number of unique DOM $_{HC}$ molecular formulae produced from oil+ISB (n = 2296) relative to the number of unique formulae in DOM $_{HC}$ from oil (n = 373) (Fig. 4a-b, Table S2). The addition of OP40 resulted in a nearly 12-fold increase in the number of DOM $_{HC}$ formulae that were produced after ISB (n = 2727) relative to those in the samples prior to ISB (n = 231) (Fig. 4c-d, Table S2). In both cases, the unique formulae produced after ISB cover a broad compositional range, with a high density of aliphatic formulae and those consistent with CRAM. This result indicates that there are both labile and refractory DOM $_{HC}$ compounds produced after ISB.

Fig. 4f-i show van Krevelen diagrams of the DOM $_{HC}$ formulae unique to 0-day oil+ISB and oil+OP40+ISB compared with the DOM $_{HC}$ for each sample after the 28-day microbial incubation. There is approximately a

2.6-fold decrease in the number of unique molecular formulae in the sample after 28 days of incubation for the oil+ISB. The oil+OP40+ISB sample exhibited a two-fold decrease in the number of unique molecular formulae following 28 days of incubation. In both cases, the selectively removed formulae tend to be relatively aliphatic in nature. This result is consistent with previous reports regarding the lability of relatively aliphatic DOM compounds (Podgorski et al., 2021; D'Andrilli et al., 2015; Spencer et al., 2014). In the absence of herder, the "produced" are selectively preserved formulae after 28-days of incubation tend to be aromatic in nature. The samples with herder show both aromatic and aliphatic type compounds formed or preserved after 28-days of incubation. Biotic and abiotic degradation of both aliphatic and aromatics that are produced by ISB is the subject of future studies.

3.6. Microbial community analyses

Quality filtering resulted in a total of 112,897 high-quality sequences in 46 samples. Samples contained an average of 2454 \pm 2496 SE sequences with a range of 186–14,497 sequences. Rarefaction to 999 sequences/sample resulted in the exclusion of seven samples due to low sequencing yields (See Table S3 for excluded samples)

3.6.1. Alpha diversity

We calculated three alpha diversity indices: Observed number of ASVs, Shannon's H, and Faith's Phylogenetic Diversity (Figure S2). Shannon's index combines measurements of both richness and evenness, while PD includes a phylogenetic component by comparing the total length of all phylogenetic branches among members of a community. Observed ASVs and Shannon indices differed significantly among treatments (Observed: ANOVA: $F_{4.33} = 7.72$, p < 0.001; Shannon: ANOVA: $F_{4,33} = 4.94$, p = 0.003), but not PD (ANOVA: $F_{4,33} = 2.25$, p = 0.09; For pairwise comparisons of all treatments for all alpha diversity indices see Table S4). Sampling day did not significantly affect Observed ASVs and Shannon indices (p = 0.108, p = 0.156), but did differ for the PD (ANOVA: $F_{1,36}=8.13$, p=0.007), indicating that despite changes in the community over time, the richness and evenness of the microbiome remained the same. Bacterial diversity was found to be lower in sea ice and water contaminated with crude oil than in control groups (Brakstad et al., 2008; Morris et al., 2018); a result that contradicts the findings of this study. Pearson's correlation analysis of abundance data (observed ASVs and Shannon's H) against each chemical factor did not identify significant correlations with any of these variables. All confidence intervals overlapped with 0 and p > 0.05 in all cases (Table S7)

3.6.2. Betadiversity

Samples clustered into two groups along PCoA Axis 1, which explained 46.8% of the total variance among samples along that axis (Fig. 5). Samples collected on day 0 and 4 clustered together, while samples collected on day 28 clustered separately (Fig. 5A). For amongtreatment comparisons, community composition differed significantly (Permanova: $p = \langle 0.001-0.011 \rangle$, and also sampling day was a significant factor (Permanova: p < 0.001) for all distance matrices (Table S5). Sampling day explained 33.8-63.6% of the variation in microbial community, compared to 11.9-19.3% explained by treatment (Table 1). Pairwise comparisons showed that all sampling days significantly differed from each other in microbial composition (Table S6), and that the significance of treatments was driven by the differences between Seawater and Oil+OP-40 (p_{adjb} = 0.02; Table S8). Distance from the sample cloud centroid (betadispersion) significantly differed among samplings days, but not among treatments (Permutation test for homogeneity of multivariate dispersions: $F_{2,42} = 9.86$, p < 0.001; $F_{4,28} =$ 0.16, p = 0.958).

The two distinct sample clusters in our PCoA correlated with Aromatic contribution, with samples collected on day 0 and 4 having relatively high levels, compared to low levels on day 28 (Fig. 5B). Within the

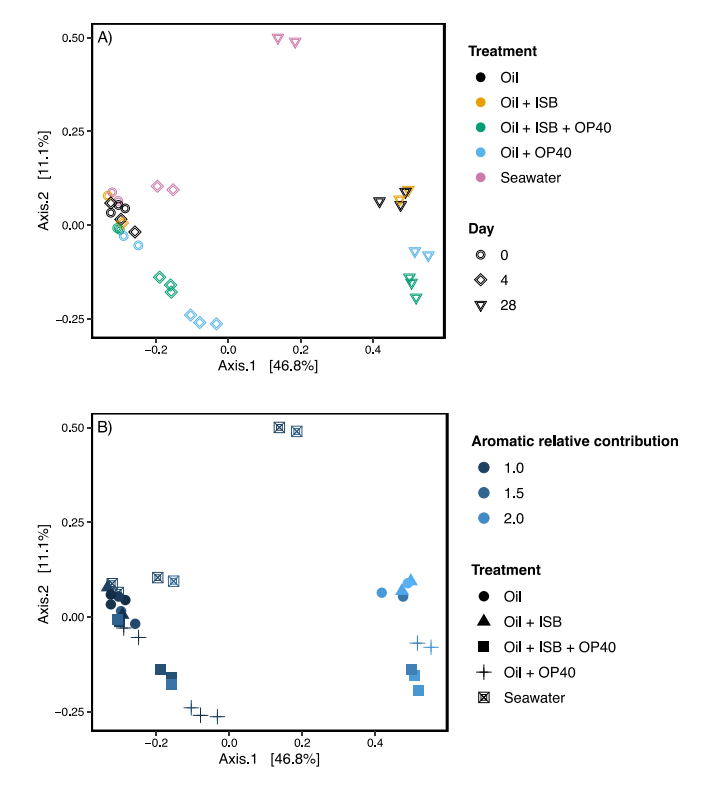


Fig. 5. Principal Coordinates Analysis of A) Bray-Curtis distance matrix from bacterial communities subjected to different treatments on different sampling days, and B) relative contribution of aromatics.

 Table 1

 Permutational Multivariate Analysis of Variance of a Bray-Curtis distance matrix of seawater microbiomes for different components of DOM_{HC} .

	F _{1,29}	R ²	p
Total Aromatics	18.7	0.353	< 0.001
Aliphatics	2.15	0.04	0.058
Unsaturated low OC	1.91	0.036	0.087
Unsaturated high OC	1.29	0.024	0.224

DOC class, the relative contribution of aromatics significantly explained 35.3% of total variation in microbiome communities ($F_{1,29}=18.70$, p<0.001, $R^2=0.353$; Table 1), which was ~ 10 times higher than aliphatics and unsaturated low/high oxygen content.

A previous study showed that microbial communities reverted to their original communities over time after oil contamination (Rodriguez et al., 2015), but we did not observe a similar pattern. Experimental treatments appeared to cluster more tightly at day 28, which was supported by our betadispersion result. A shift in community over time in the seawater control was also detected, which indicates that the initial microbial community may not have been stable over time. It is possible that these results mirror the natural dynamics in marine microbial communities, but to our knowledge no studies have examined natural communities at the same location over a time frame of days.

3.6.3. Community composition

Microbiomes in all treatments were dominated by Proteobacteria, followed by Bacteroidetes and Cyanobacteria (Fig. S3A). Within the Proteobacteria, genus composition differed greatly per treatment with no clear visual pattern (Fig. S3B). Seawater had a significantly lower abundance of *Marinomonas* compared to all treatments (Fig. 6). *Marinomonas* is a genus of psychrotolerant, aerobic bacteria that have been previously isolated from water and sediments in the Arctic and Antarctic (Gupta et al., 2006; Zhang et al., 2008; Gontikaki et al., 2018).

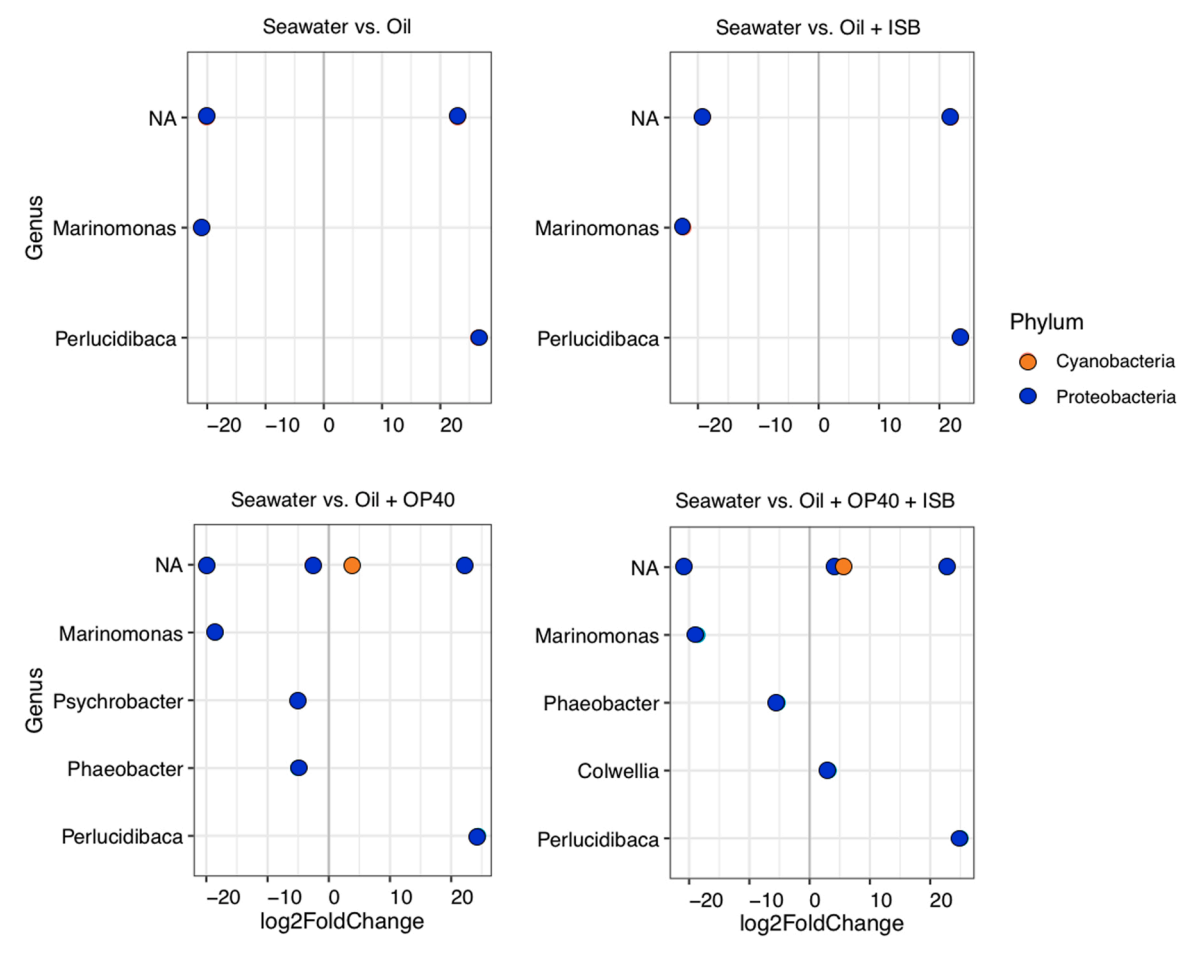


Fig. 6. Observed changes in bacterial genus abundance. Each comparison is between control (seawater) and treatment (Oil, Oil + ISB, Oil + OP40, and Oil + OP40 + ISB). Positive log_2 fold changes indicate a higher relative abundance is present in the seawater control, while negative values indicate a higher relative abundance is present in the respective treatment. NA includes sequences that could not be confidently classified to genus level. Colors represent phyla (orange = cyanobacteria, blue = proteobacteria). Changes are considered different for an adjusted p-value < 0.05.

Marinomonas sp. were found to contain a number of genes related to the degradation of aromatic hydrocarbons(Liao et al., 2015) and its family, Oceanospirillaceae, dominated microbial communities in seawater contaminated with crude oil (Morris et al., 2018). Marinomonas sp. were also more abundant in sea ice samples contaminated with crude oil than clean ice and in seawater contaminated with crude oil (Brakstad et al., 2008; Salerno et al., 2018).

Contrastingly, a lower relative abundance of *Perlucidibaca* sp. (Fam. Moraxellaceae) was detected in all treatments compared to the Seawater control. Perlucidibaca sp. are known hydrocarbon degraders, and this result therefore was unexpected (Lofthus et al., 2020). However, these results did not support this potential function due the lower abundance of *Perlicidibaca* sp. detected in the samples. We also postulate that ISB+OP-40 may have reduced the oxygen content of water, which would limit the growth potential of aerobe bacteria. Both *Marinomonas* sp. and *Perlucidibaca* sp. show similar patterns in differential abundance in all treatments, including the addition of only oil, indicating that the additional OP-40 and ISB clean-up methods did not affect the shifts in these genera. *Phaeobacter* sp. were significantly more abundant in treatments containing OP-40. The *Phaeobacter* genus contains species that are associated with hydrocarbon degradation, and are strict aerobes or facultative anaerobes (Bacosa et al., 2018).

4. Conclusions

This study identified that ISB, both with and without the addition of OP-40, has a significant impact on both the DOM_{HC} chemical

composition and 16s rRNA seawater microbial community diversity, compared to non-combusted oiled seawater. Oil+ISB selected for *Marinomonas* and *Perlucidibaca*, which are known hydrocarbon degraders, and the abundance of these genera were driven primarily by relative aromatic percentage in DOM_{HC} . Herder application and ISB induces a unique molecular signature that is represented in FT-ICR MS and optical measurements. We postulate the composition of DOM_{HC} contains oxidized non-aromatics and/or CRAM (carboxyl rich alicyclic molecules) formed either by combustion and/or physical partitioning associated with enhanced solubility of these fractions, e.g., higher burn temperatures of OP-40+ISB. Overall, ISB had the greatest impact on aromatic and condensed aromatic DOM_{HC} content, and the microbial community diversity shift was consistent with this scenario. This information helps further toxicological considerations due to exposure of these ISB-derived aromatic and condensed aromatics.

$CRediT\ authorship\ contribution\ statement$

Patrick Tomco: Conceptualization, Methodology, Data curation, Writing – original draft, Writing – review & editing, Supervision, Funding acquisition. Khrystyne Duddleston: Conceptualization, Methodology, Writing – review & editing, Supervision, Funding acquisition. Adrienne Driskill: Methodology, Validation, Formal analysis, Investigation, Writing – review & editing. Jasmine J Hatton: Methodology, Validation, Resources, Software, Visualization. Kirsten Grond: Software, Formal analysis, Data curation, Writing – original draft, Writing – review & editing, Visualization. Toshia Wrenn: Methodology,

Validation, Data curation, Writing – original draft, Visualization. **Matthew Tarr:** Supervision, Resources. **David Podgorski:** Software, Validation, Formal analysis, Resources, Data curation, Writing – original draft, Writing – review & editing, Visualization. **Phoebe Zito:** Conceptualization, Methodology, Software, Validation, Formal analysis, Investigation, Resources, Data curation, Writing – review & editing, Visualization

Declaration of Competing Interest

The authors declare that they have no known competing financial interests or personal relationships that could have appeared to influence the work reported in this paper.

Acknowledgements

Funding from this project was provided by the UAA ConocoPhillips Arctic Science and Engineering Endowment to P Tomco and the National Science Foundation award #1929173. A portion of this work was performed at the National High Magnetic Field Laboratory ICR User Facility, which is supported by the National Science Foundation Division of Chemistry through DMR-1644779 and the State of Florida.

Appendix A. Supporting information

Supplementary data associated with this article can be found in the online version at doi:10.1016/j.jhazmat.2021.127598.

References

- Aeppli, C., Carmichael, C., Nelson, R.K., Lemkau, K.L., Graham, W.M., Redmond, M.C., Valentine, D.L., Reddy, C.M., 2012. Oil weathering after the deepwater horizon disaster led to the formation of oxygenated residues. Environ. Sci. Technol. 46, 8799–8807.
- Aeppli, C., Nelson, R.K., Carmichael, C.A., Arakawa, N., Aluwihare, L.I., Valentine, D.L., Reddy, C.M., 2013. Characterization of Recalcitrant Oxygenated Hydrocarbons Formed upon Oil Weathering after the Deepwater Horizon Disaster. American Chemical Society. GEOC150.
- Amir, A., McDonald, D., Navas-Molina Jose, A., Kopylova, E., Morton James, T., Zech Xu, Z., Kightley Eric, P., Thompson Luke, R., Hyde Embriette, R., Gonzalez, A., Knight, R., Gilbert Jack, A., 2017. Deblur rapidly resolves single-nucleotide community sequence patterns. mSystems 2, e00191–00116.
- Bacosa, H.P., Erdner, D.L., Rosenheim, B.E., Shetty, P., Seitz, K.W., Baker, B.J., Liu, Z., 2018. Hydrocarbon degradation and response of seafloor sediment bacterial community in the Northern Gulf of Mexico to Light Louisiana Sweet crude oil. ISME 12, 2532–2543.
- Bao, M.-t, Wang, L.-n, Sun, P.-y, Cao, L.-x, Zou, J., Li, Y.-m, 2012. Biodegradation of crude oil using an efficient microbial consortium in a simulated marine environment. Mar. Pollut. Bull. 64, 1177–1185.
- Bekins, B.A., Cozzarelli, I.M., Erickson, M.L., Steenson, R.A., Thorn, K.A., 2016. Crude oil metabolites in groundwater at two spill sites. Groundwater 54, 681–691.
- Benjamini, Y., Hochberg, Y., 1995. Controlling the false discovery rate: a practical and powerful approach to multiple testing. J. R. Stat. Soc. Ser. B Stat. Method. J. R. Stat. 57, 289–300.
- Bera, G., Doyle, S., Passow, U., Kamalanathan, M., Wade, T.L., Sylvan, J.B., Sericano, J. L., Gold, G., Quigg, A., Knap, A.H., 2020. Biological response to dissolved versus dispersed oil. Mar. Pollut. Bull. 150, 110713.
- Bianchi, T.S., Osburn, C., Shields, M.R., Yvon-Lewis, S., Young, J., Guo, L.D., Zhou, Z.Z., 2014. Deepwater horizon oil in Gulf of Mexico waters after 2 years: transformation into the dissolved organic matter pool. Environ. Sci. Technol. 48, 9288–9297.
- Bokulich, N.A., Kaehler, B.D., Rideout, J.R., Dillon, M., Bolyen, E., Knight, R., Huttley, G. A., Gregory Caporaso, J., 2018. Optimizing taxonomic classification of marker-gene amplicon sequences with QIIME 2's q2-feature-classifier plugin. Microbiome 6, 90.
- Bolyen, E., Rideout, J.R., Dillon, M.R., Bokulich, N.A., Abnet, C.C., Al-Ghalith, G.A., Alexander, H., Alm, E.J., Arumugam, M., Asnicar, F., Bai, Y., Bisanz, J.E., Bittinger, K., Brejnrod, A., Brislawn, C.J., Brown, C.T., Callahan, B.J., Caraballo-Rodríguez, A.M., Chase, J., Cope, E.K., Da Silva, R., Diener, C., Dorrestein, P.C., Douglas, G.M., Durall, D.M., Duvallet, C., Edwardson, C.F., Ernst, M., Estaki, M., Fouquier, J., Gauglitz, J.M., Gibbons, S.M., Gibson, D.L., Gonzalez, A., Gorlick, K., Guo, J., Hillmann, B., Holmes, S., Holste, H., Huttenhower, C., Huttley, G.A., Janssen, S., Jarmusch, A.K., Jiang, L., Kaehler, B.D., Kang, K.B., Keefe, C.R., Keim, P., Kelley, S.T., Knights, D., Koester, I., Kosciolek, T., Kreps, J., Langille, M.G.I., Lee, J., Ley, R., Liu, Y.-X., Loftfield, E., Lozupone, C., Maher, M., Marotz, C., Martin, B.D., McDonald, D., McIver, L.J., Melnik, A.V., Metcalf, J.L., Morgan, S.C., Morton, J.T., Naimey, A.T., Navas-Molina, J.A., Nothias, L.F., Orchanian, S.B., Pearson, T., Peoples, S.L., Petras, D., Preuss, M.L., Pruesse, E., Rasmussen, L.B., Rivers, A., Robeson, M.S., Rosenthal, P., Segata, N., Shaffer, M., Shiffer, A., Sinha, R., Song, S.J.,

- Spear, J.R., Swafford, A.D., Thompson, L.R., Torres, P.J., Trinh, P., Tripathi, A., Turnbaugh, P.J., Ul-Hasan, S., van der Hooft, J.J.J., Vargas, F., Vázquez-Baeza, Y., Vogtmann, E., von Hippel, M., Walters, W., Wan, Y., Wang, M., Warren, J., Weber, K. C., Williamson, C.H.D., Willis, A.D., Xu, Z.Z., Zaneveld, J.R., Zhang, Y., Zhu, Q., Knight, R., Caporaso, J.G., 2019. Reproducible, interactive, scalable and extensible microbiome data science using QIIME 2. Nat. Biotechnol. 37, 852–857.
- Boström, K.H., Simu, K., Hagström, Å., Riemann, L., 2004. Optimization of DNA extraction for quantitative marine bacterioplankton community. Anal. Limnol. Oceano - Meth. 2, 365–373.
- Brakstad, O.G., Nonstad, I., Faksness, L.G., Brandvik, P.J., 2008. Responses of microbial communities in Arctic sea ice after contamination by crude petroleum oil. Micro Ecol. 55, 540–552.
- Bray, J.R., Curtis, J.T., 1957. An ordination of the upland forest communities of Southern Wisconsin. Ecol. Monogr. 27, 325–349.
- Bruckberger, M.C., Morgan, M.J., Bastow, T.P., Walsh, T., Prommer, H., Mukhopadhyay, A., Kaksonen, A.H., Davis, G.B., Puzon, G.J., 2020. Investigation into the microbial communities and associated crude oil-contamination along a Gulf War impacted groundwater system in Kuwait. Water Res. 170, 115314.
- Bugden, J.B., Yeung, C.W., Kepkay, P.E., Lee, K., 2008. Application of ultraviolet fluorometry and excitation-emission matrix spectroscopy (EEMS) to fingerprint oil and chemically dispersed oil in seawater. Mar. Pollut. Bull. 56, 677–685.
- Buist, I., Cooper, D., Trudel, K., Fritt-Rasmussen, J., Wegeberg, S., Gustavson, K., Lassen, P., Alva, R., Jomaas, G., Zabilansky, L., 2018. Research investigations into herder fate, effects and windows-of-opportunity. Draft Report to Arctic Oil Spill Response Technology Joint Industry Programme (JIP), pp. 1–156.
- I. Buist, J. Morrison, Research on using oil herding surfactants to thicken oil slicks in pack ice for in situ burning, in: Proceedings of the Twenty-Eighth AMOP Technical Seminar 2005, pp. 349–375.
- I. Buist, T. Nedwed, J. Mullin, Herding agents thicken oil spills in drift ice to facilitate in situ burning: a new trick for an old dog, in: In International Oil Spill Conference American Petroleum Institute, 2008, pp. 673–679.
- I. Buist, S. Potter, R. Belore, A. Guarino, P. Meyer, J. Mullin, Employing chemical herders to improve other marine oil spill response operations, In Proceedings of the Thirty-Third AMOP Technical Seminar on Environmental Contamination and Response, Environment Canada, Ottawa 2010a, pp. 1109–1134.
- Buist, I., Potter, S., Nedwed, T., Mullin, J., 2011. Herding surfactants to contract and thicken oil spills in pack ice for in situ burning. Cold Reg. Sci. Technol. 67, 3–23.
- I. Buist, S. Potter, S.E. Sørstrøm, Barents sea field test of herder to thicken oil for in situ burning in drift ice, In Proceedings of the Thirty-Third AMOP Technical Seminar on Environmental Contamination and Response, Ottawa: Environment Canada, 2010b, pp. 725–742.
- I. Buist, S. Potter, L. Zabilansky, P. Meyer, J. Mullin, Mid-scale test tank research on using oil herding surfactants to thicken oil slicks in pack ice: an update, In Proceedings Arctic and Marine Oilspill Program Technical Seminar 2006, pp. 691–709.
- Bullock, R.J., Aggarwal, S., Perkins, R.A., Schnabel, W., 2017. Scale-up considerations for surface collecting agent assisted in-situ burn crude oil spill response experiments in the Arctic: Laboratory to field-scale investigations. J. Environ. Manag. 190, 266–273
- Bullock, R.J., Perkins, R.A., Aggarwal, S., 2019. In-situ burning with chemical herders for Arctic oil spill response: Meta-analysis and review. Sci. Total Environ. 675, 705–716. Campbell, R.W., 2018. Hydrographic trends in Prince William Sound, Alaska,
- 1960–2016. Deep Sea Res. Part II Top. Stud. Oceano 147, 43–57.
- Caporaso, J.G., Lauber, C.L., Walters, W.A., Berg-Lyons, D., Huntley, J., Fierer, N., Owens, S.M., Betley, J., Fraser, L., Bauer, M., Gormley, N., Gilbert, J.A., Smith, G., Knight, R., 2012. Ultra-high-throughput microbial community analysis on the Illumina HiSeq and MiSeq platforms. ISME 6, 1621–1624.
- Coble, P.G., 1996. Characterization of marine and terrestrial DOM in seawater using excitation-emission matrix spectroscopy. Mar. Chem. 51, 325–346.
- Corilo, Y., 2015. EnviroOrg. Florida State University, Tallahassee.
- Cory, R.M., McKnight, D.M., 2005. Fluorescence spectroscopy reveals ubiquitous presence of oxidized and reduced quinones in dissolved organic matter. Environ. Sci. Technol. 39, 8142–8149.
- D'Andrilli, J., Cooper, W.T., Foreman, C.M., Marshall, A.G., 2015. An ultrahighresolution mass spectrometry index to estimate natural organic matter lability. Rapid Commun. Mass Spectrom. 29, 2385–2401.
- Davis, J., Benner, R., 2007. Quantitative estimates of labile and semi-labile dissolved organic carbon in the western arctic ocean: a molecular approach. Limnol. Oceanogr. 52, 2434–2444.
- Dittmar, T., Koch, B., Hertkorn, N., Kattner, G., 2008. A simple and efficient method for the solid-phase extraction of dissolved organic matter (SPE-DOM) from seawater. Limnol. Oceano -Meth. 6, 230–235.
- Dong, C., Bai, X., Sheng, H., Jiao, L., Zhou, H., Shao, Z., 2015. Distribution of PAHs and the PAH-degrading bacteria in the deep-sea sediments of the high-latitude Arctic Ocean. Biogeosciences 12, 2163–2177.
- Dunn, O.J., 1961. Multiple comparisons among means. J. Am. Stat. Assoc. 56, 52–64.Dvorski, S.E.M., Gonsior, M., Hertkorn, N., Uhl, J., Muller, H., Griebler, C., Schmitt-Kopplin, P., 2016. Geochemistry of dissolved organic matter in a spatially highly resolved groundwater petroleum hydrocarbon plume cross-section. Environ. Sci. Technol. 50, 5536–5546.
- D'Andrilli, J., Junker, J.R., Smith, H.J., Scholl, E.A., Foreman, C.M., 2019. DOM composition alters ecosystem function during microbial processing of isolated sources. Biogeochemistry 142, 281–298.
- Essaid, H.I., Bekins, B.A., Herkelrath, W.N., Delin, G.N., 2011. Crude oil at the Bemidji site: 25 years of monitoring, modeling, and understanding. Ground Water 49, 706–726.

- Faith, D.P., 1992. Conservation evaluation and phylogenetic diversity. Biol. Conserv. 61, 1–10.
- Fellman, J.B., Hood, E., Spencer, R.G.M., 2010. Fluorescence spectroscopy opens new windows into dissolved organic matter dynamics in freshwater ecosystems: a review. Limnol. Oceanogr. 55, 2452–2462.
- M. Fingas, Review of oil spill herders. PWS-RCAC Report, in, (http://www.pwsrcac.org/wp-content/uploads/filebase/board_meetings/2014-01-23_board_meeting/3 -05-Attachment%20A-Review%20of%20Oil%20Spill%20Herders.pdf), 2013.
- M. Fingas, Polar compounds in oils and their aquatic toxicity, in: International Oil Spill Conference Proceedings, 2017, pp. 2017036.
- Fingas, M., 2018. In-Situ Burning an Update. In: In-Situ Burning for Oil Spill Countermeasures. CRC Press, pp. 1–171.
- Fritt-Rasmussen, J., Wegeberg, S., Gustavson, K., 2015. Review on burn residues from in situ burning of oil spills in relation to Arctic waters. Water Air Soil Pollut. 226, 329.
- Gallego, S., Vila, J., Tauler, M., Nieto, J.M., Breugelmans, P., Springael, D., Grifoll, M., 2014. Community structure and PAH ring-hydroxylating dioxygenase genes of a marine pyrene-degrading microbial consortium. Biodegradation 25, 543–556.
- Gerdes, B., Brinkmeyer, R., Dieckmann, G., Helmke, E., 2005. Influence of crude oil on changes of bacterial communities in arctic sea-ice. FEMS Microbiol. Ecol. 53, 129–139.
- Gilbert, J.A., Meyer, F., Antonopoulos, D., Balaji, P., Brown, C.T., Brown, C.T., Desai, N., Eisen, J.A., Evers, D., Field, D., Feng, W., Huson, D., Jansson, J., Knight, R., Knight, J., Kolker, E., Konstantindis, K., Kostka, J., Kyrpides, N., Mackelprang, R., McHardy, A., Quince, C., Raes, J., Sczyrba, A., Shade, A., Stevens, R., 2010. Meeting report: the terabase metagenomics workshop and the vision of an Earth microbiome project. Stand Genom. Sci. 3, 243–248.
- Gonçalves-Araujo, R., Granskog, M.A., Bracher, A., Azetsu-Scott, K., Dodd, P.A., Stedmon, C.A., 2016. Using fluorescent dissolved organic matter to trace and distinguish the origin of Arctic surface waters. Sci. Rep. 6, 33978.
- Gonsior, M., Valle, J., Schmitt-Kopplin, P., Hertkorn, N., Bastviken, D., Luek, J., Harir, M., Bastos, W., Enrich-Prast, A., 2016. Chemodiversity of dissolved organic matter in the Amazon basin. Biogeosciences 13, 4279–4290.
- Gontikaki, E., Potts, L.D., Anderson, J.A., Witte, U., 2018. Hydrocarbon-degrading bacteria in deep-water subarctic sediments (Faroe-Shetland Channel). J. Appl. Microbiol. 125, 1040–1053.
- Goranov, A.I., Wozniak, A.S., Bostick, K.W., Zimmerman, A.R., Mitra, S., Hatcher, P.G., 2021. Labilization and diversification of pyrogenic dissolved organic matter by microbes. Biogeosciences Discuss. 2021, 1–31.
- Gupta, P., Chaturvedi, P., Pradhan, S., Delille, D., Shivaji, S., 2006. Marinomonas Polaris Sp. Nov., a psychrohalotolerant strain isolated from coastal sea water off the subantarctic Kerguelen. Isl. Int. J. Syst. Evol. Microbiol 56, 361–364.
- Hansen, A.M., Kraus, T.E.C., Pellerin, B.A., Fleck, J.A., Downing, B.D., Bergamaschi, B.A., 2016. Optical properties of dissolved organic matter (DOM): effects of biological and photolytic degradation. Limnol. Oceanogr. 61, 1015–1032.
- Han, X., Scott, A.C., Fedorak, P.M., Bataineh, M., Martin, J.W., 2008. Influence of molecular structure on the biodegradability of naphthenic acids. Environ. Sci. Technol. 42, 1290–1295.
- Harriman, B.H., Zito, P., Podgorski, D.C., Tarr, M.A., Suflita, J.M., 2017. Impact of photooxidation and biodegradation on the fate of oil spilled during the deepwater horizon incident: advanced stages of weathering. Environ. Sci. Technol. 51, 7412–7421.
- Harshman, R., 1984. How Can I Know if it's Real?" A Catalog of Diagnostics for use with Three-Mode Factor Analysis and Multidimensional Scaling. In: Law, H.G., Snyder, C. W., Hattie, J.A., McDonald, R.P. (Eds.), Research Methods for Multimode Data Analysis. Praeger Publishers Inc, pp. 566–591.
- Hawkes, J.A., D'Andrilli, J., Sleighter, R.L., Chen, H., Hatcher, P.G., Ijaz, A., Khaksan, M., Schum, S., Mazzoleni, L., Chu, R., Tolic, N., Kew, W., Hess, N., Lv, J., Zhang, S., Chen, H., Shi, Q., Hutchins, R.H.S., Lozano, D.C.P., Gavard, R., Jones, H.E., Thomas, M.J., Barrow, M., Osterholz, H., Dittmar, T., Simon, C., Gleixner, G., Berg, S.M., Remucal, C.K., Catalán, N., Cole, R.B., Noreiga-Ortega, B., Singer, G., Radoman, N., Schmitt, N.D., Stubbins, A., Agar, J.N., Zito, P., Podgorski, D.C., 2020. An international laboratory comparison of dissolved organic matter composition by high resolution mass spectrometry: are we getting the same answer? Limnol. Oceano Meth.
- Hertkorn, N., Benner, R., Frommberger, M., Schmitt-Kopplin, P., Witt, M., Kaiser, K., Kettrup, A., Hedges, J.I., 2006. Characterization of a major refractory component of marine dissolved organic matter. Geochim. Cosmochim. Acta 70, 2990–3010.
- Hervé, M., 2018. RVAideMemoire: testing and plotting procedures for biostatistics. R. Package Version 0. 9-69 3.
- He, C., Zhang, Y., Li, Y., Zhuo, X., Li, Y., Zhang, C., Shi, Q., 2020. In-house standard method for molecular characterization of dissolved organic matter by FT-ICR mass spectrometry. ACS Omega 5, 11730–11736.
- Jaggi, A., Radović, J.R., Snowdon, L.R., Larter, S.R., Oldenburg, T.B.P., 2019. Composition of the dissolved organic matter produced during in situ burning of spilled oil. Org. Geochem. 138, 103926.
- Katoh, K., Standley, D.M., 2013. MAFFT multiple sequence alignment software version 7: improvements in performance and usability. Mol. Biol. Evol. 30, 772–780.
- King, G.M., Kostka, J.E., Hazen, T.C., Sobecky, P.A., 2015. Microbial responses to the Deepwater Horizon oil spill: from coastal wetlands to the deep sea. Ann. Rev. Mar. Sci. 7, 377–401.
- King, S.M., Leaf, P.A., Olson, A.C., Ray, P.Z., Tarr, M.A., 2014. Photolytic and photocatalytic degradation of surface oil from the deepwater horizon spill. Chemosphere 95, 415–422.
- Kleindienst, S., Paul, J.H., Joye, S.B., 2015. Using dispersants after oil spills: impacts on the composition and activity of microbial communities. Nat. Rev. Microbiol. 13, 388–396.

- Koch, B.P., Dittmar, T., 2006. From mass to structure: an aromaticity index for highresolution mass data of natural organic matter. Rapid Commun. Mass Spectrom. 20, 926–932
- Kothawala, D.N., Stedmon, C.A., Müller, R.A., Weyhenmeyer, G.A., Köhler, S.J., Tranvik, L.J., 2014. Controls of dissolved organic matter quality: evidence from a large-scale Boreal lake survey. Glob. Change Biol. 20, 1101–1114.
- Kowalczuk, P., Cooper, W.J., Whitehead, R.F., Durako, M.J., Sheldon, W., 2003. Characterization of CDOM in an Organic-Rich River and surrounding coastal ocean in the South Atlantic bight. Aquat. Sci. 65, 384–401.
- Kowalczuk, P., Tilstone, G.H., Zabłocka, M., Röttgers, R., Thomas, R., 2013. Composition of dissolved organic matter along an Atlantic Meridional transect from fluorescence spectroscopy and parallel factor analysis. Mar. Chem. 157, 170–184.
- Lamendella, R., Strutt, S., Borglin, S., Chakraborty, R., Tas, N., Mason, O.U., Hultman, J., Prestat, E., Hazen, T.C., Jansson, J.K., 2014. Assessment of the Deepwater Horizon oil spill impact on Gulf coast microbial communities. Front Microbiol 5, 130.
- Lapierre, J.F., del Giorgio, P.A., 2014. Partial coupling and differential regulation of biologically and photochemically labile dissolved organic carbon across boreal aquatic networks. Biogeosciences 11, 5969–5985.
- Liao, L., Sun, X., Yu, Y., Chen, B., 2015. Draft genome of Marinomonas sp. BSi20584 from Arctic sea ice. Mar. Genom. 23, 23–25.
- Lin, Q., Mendelssohn, I.A., 2009. Potential of restoration and phytoremediation with Juncus roemerianus for diesel-contaminated coastal wetlands. Ecol. Eng. 35, 85–91.
- Lofthus, S., Bakke, I., Tremblay, J., Greer, C.W., Brakstad, O.G., 2020. Biodegradation of weathered crude oil in seawater with frazil ice. Mar. Pollut. Bull. 154, 111090.
- Love, M.I., Huber, W., Anders, S., 2014. Moderated estimation of fold change and dispersion for RNA-Aeq data with DESeq2. Genome Biol. 15, 550.
- Lozupone, C., Knight, R., 2005. UniFrac: a new phylogenetic method for comparing microbial communities. Appl. Environ. Microbiol 71, 8228–8235.
- McDonald, D., Price, M.N., Goodrich, J., Nawrocki, E.P., DeSantis, T.Z., Probst, A., Andersen, G.L., Knight, R., Hugenholtz, P., 2012. An improved greengenestaxonomy with explicit ranks for ecological and evolutionary analyses ofbacteria and archaea. ISME 6, 610–618.
- McFarlin, K.M., Prince, R.C., Perkins, R., Leigh, M.B., 2014. Biodegradation of dispersed oil in Arctic seawater at -1°C. PLoS One 9, e84297.
- McGuire, J.T., Cozzarelli, I.M., Bekins, B.A., Link, H., Martinović-Weigelt, D., 2018. Toxicity assessment of groundwater contaminated by petroleum hydrocarbons at a well-characterized, aged, crude oil release site. Environ. Sci. Technol. 52, 12172–12178.
- McKenna, A.M., Nelson, R.K., Reddy, C.M., Savory, J.J., Kaiser, N.K., Fitzsimmons, J.E., Marshall, A.G., Rodgers, R.P., 2013. Expansion of the analytical window for oil spill characterization by ultrahigh resolution mass spectrometry: beyond gas chromatography. Environ. Sci. Technol. 47, 7530–7539.
- McKnight, D.M., Boyer, E.W., Westerhoff, P.K., Doran, P.T., Kulbe, T., Andersen, D.T., 2001. Spectrofluorometric characterization of dissolved organic matter for indication of precursor organic material and aromaticity. Limnol. Oceanogr. 46, 38–48.
- McMurdie, P.J., Holmes, S., 2013. phyloseq: an R package for reproducible interactive analysis and graphics of microbiome census data. PLOS ONE 8, e61217.
- Mirnaghi, F.S., Pinchin, N.P., Yang, Z., Hollebone, B.P., Lambert, P., Brown, C.E., 2019. Monitoring of polycyclic aromatic hydrocarbon contamination at four oil spill sites using fluorescence spectroscopy coupled with parallel factor-principal component analysis. Environ. Sci.: Process. Impacts 21, 413–426.
- Morris, L., O'Brien, A., Natera, S.H.A., Lutz, A., Roessner, U., Long, S.M., 2018. Structural and functional measures of marine microbial communities: an experiment to assess implications for oil spill management. Mar. Pollut. Bull. 131, 525–529.
- Murphy, K.R., Ruiz, G.M., Dunsmuir, W.T.M., Waite, T.D., 2006. Optimized parameters for fluorescence-based verification of ballast water exchange by ships. Environ. Sci. Technol. 40, 2357–2362.
- Murphy, K.R., Stedmon, C.A., Graeber, D., Bro, R., 2013. Fluorescence spectroscopy and multi-way techniques. PARAFAC. Anal. Methods 5, 6557.
- Murphy, K.R., Stedmon, C.A., Wenig, P., Bro, R., 2014. OpenFluor– an online spectral library of auto-fluorescence by organic compounds in the environment. Anal. Methods 6, 658–661.
- O'Donnell, J.A., Aiken, G.R., Butler, K.D., Guillemette, F., Podgorski, D.C., Spencer, R.G. M., 2016. D.O.M. Composition and transformation in boreal forest soils: the effects of temperature and organic-horizon decomposition state. J. Geophys. Res. Biogeosci. 121, 2727–2744.
- Ohno, T., 2002. Fluorescence inner-fltering correction for determining the humification index of dissolved organic matter. Environ. Sci. Technol. 36, 742–746.
- Ohno, T., Chorover, J., Omoike, A., Hunt, J., 2007. Molecular weight and humification index as predictors of adsorption for plant- and manure-derived dissolved organic matter to goethite. Eur. J. Soil Sci. 58, 125–132.
- J. Oksanen, F.G. Blanchet, M. Friendly, R. Kindt, P. Legendre, D. McGlinn, P.R. Minchin, R. O'Hara, G. Simpson, P. Solymos, Vegan: Community Ecology Package. R Package Version 2.5–6. 2019, in, 2020.
- Olson, G.M., Gao, H., Meyer, B.M., Miles, M.S., Overton, E.B., 2017. Effect of Corexit 9500A on Mississippi canyon crude oil weathering patterns using artificial and natural seawater. Heliyon 3, e00269.
- Parlanti, E., Wörz, K., Geoffroy, L., Lamotte, M., 2000. Dissolved organic matterfluorescence spectroscopy as a tool to estimate biological activity in acoastal zone submitted to anthropogenic inputs. Org. Geochem. 31, 1765–1781.
- Podgorski, D.C., Zito, P., Kellerman, A.M., Bekins, B.A., Cozzarelli, I.M., Smith, D.F., Cao, X., Schmidt-Rohr, K., Wagner, S., Stubbins, A., Spencer, R.G.M., 2021. Hydrocarbons to carboxyl-rich alicyclic molecules: a continuum model to describe biodegradation of petroleum-derived dissolved organic matter in contaminated groundwater plumes. J. Hazard. Mater. 402, 123998.

- Podgorski, D.C., Zito, P., McGuire, J.T., Martinovic-Weigelt, D., Cozzarelli, I.M., Bekins, B.A., Spencer, R.G.M., 2018. Examining natural attenuation and acute toxicity of petroleum-derived dissolved organic matter with optical spectroscopy. Environ. Sci. Technol. 52, 6157–6166.
- Price, M.N., Dehal, P.S., Arkin, A.P., 2010. FastTree 2 approximately maximum-likelihood trees for large alignments. PLoS One 5, e9490.
- Prince, R.C., McFarlin, K.M., Butler, J.D., Febbo, E.J., Wang, F.C., Nedwed, T.J., 2013.

 The primary biodegradation of dispersed crude oil in the sea. Chemosphere 90, 521–526
- Ray, P.Z., Chen, H., Podgorski, D.C., McKenna, A.M., Tarr, M.A., 2014. Sunlight creates oxygenated species in water-soluble fractions of deepwater horizon oil. J. Hazard. Mater. 280, 636–643.
- Retelletti Brogi, S., Kim, J.-H., Ryu, J.-S., Jin, Y.K., Lee, Y.K., Hur, J., 2019. Exploring sediment porewater Dissolved Organic Matter (DOM) in a mud volcano: clues of a thermogenic DOM source from fluorescence spectroscopy. Mar. Chem. 211, 15–24.
- Riedel, T., Biester, H., Dittmar, T., 2012. Molecular fractionation of dissolved organic matter with metal salts. Environ. Sci. Technol. 46, 4419–4426.
- Rodriguez, R.L., Overholt, W.A., Hagan, C., Huettel, M., Kostka, J.E., Konstantinidis, K. T., 2015. Microbial community successional patterns in beach sands impacted by the deepwater horizon oil spill. ISME 9, 1928–1940.
- Rojas-Alva, U., Fritt-Rasmussen, J., Jomaas, G., 2020. Experimental study of thickening effectiveness of two herders for in-situ burning of crude oils on water. Cold Reg. Sci. Technol. 175, 103083.
- Salerno, J.L., Little, B., Lee, J., Hamdan, L.J., 2018. Exposure to crude oil and chemical dispersant may impact marine microbial biofilm composition and steel corrosion. Front. Mar. Sci. 5.
- Savory, J.J., Kaiser, N.K., McKenna, A.M., Xian, F., Blakney, G.T., Rodgers, R.P., Hendrickson, C.L., Marshall, A.G., 2011. Parts-per-billion fourier transform ion cyclotron resonance mass measurement accuracy with a "Walking" calibration equation. Anal. Chem. 83, 1732–1736.
- Shannon, C.E., 1948. A mathematical theory of communication. Bell Syst. Tech. 27, 379–423.
- Smith, D.F., Podgorski, D.C., Rodgers, R.P., Blakney, G.T., Hendrickson, C.L., 2018. 21 Tesla FT-ICR Mass spectrometer for ultrahigh-resolution analysis of complex organic mixtures. Anal. Chem. 90, 2041–2047.
- Spencer, R.G.M., Bolton, L., Baker, A., 2007. Freeze/Thaw and pH effects on freshwater dissolved organic matter fluorescence and absorbance properties from a number of UK locations. Water Res. 41, 2941–2950.
- Spencer, R.G.M., Guo, W.D., Raymond, P.A., Dittmar, T., Hood, E., Fellman, J., Stubbins, A., 2014. Source and biolability of ancient dissolved organic matter in glacier and lake ecosystems on the Tibetan plateau. Geochim. Cosmochim. Acta 142, 64–74.
- Spencer, R.G.M., Kellerman, A.M., Podgorski, D.C., Macedo, M.N., Jankowski, K., Nunes, D., Neill, C., 2019. Identifying the molecular signatures of agricultural expansion in amazonian headwater streams. J. Geophys Res.-Biogeo. 124, 1637–1650.
- Stedmon, Ca, Bro, R., 2008. Characterizing dissolved organic matter fluorescence with parallel factor. Anal.: A Tutor. Limnol. Oceano -Meth 6, 572–579.
- Stout, S.A., Payne, J.R., 2016. Chemical composition of floating and sunken in-situ burn residues from the Deepwater Horizon oil spill. Mar. Pollut. Bull. 108, 186–202.
- Tan, B., Ng, C., Nshimyimana, J., Loh, L.-L., Gin, K., Thompson, J., 2015. Next-Generation Sequencing (NGS) for assessment of microbial water quality: current progress, challenges, and future opportunities. Front Microbiol. 6.

- Tfaily, M.M., Podgorski, D.C., Corbett, J.E., Chanton, J.P., Cooper, W.T., 2011. Influence of acidification on the optical properties and molecular composition of dissolved organic matter. Anal. Chim. Acta 706, 261–267.
- Tomco, P.L., Zulueta, R.C., Miller, L.C., Zito, P., Campbell, R.W., Welker, J.M., 2019. DOC export is exceeded by C fixation in may creek: a late-successional watershed of the Copper river basin, Alaska. PLoS One 14, e0225271.
- Turner, R.E., Overton, E.B., Meyer, B.M., Miles, M.S., McClenachan, G., Hooper-Bui, L., Engel, A.S., Swenson, E.M., Lee, J.M., Milan, C.S., Gao, H., 2014. Distribution and recovery trajectory of Macondo (Mississippi Canyon 252) oil in Louisiana coastal wetlands. Mar. Pollut. Bull. 87, 57–67.
- USEPA, National Contingency Plan Product Schedule, July 2021, in, (https://www.epa.gov/sites/default/files/2021-06/documents/schedule.pdf), 2021.
- USEPA, Test Methods for Evaluating Solid Wastes Physical/Chemical Methods SW-846, in, (https://www.epa.gov/hw-sw846/sw-846-compendium), 2016.
- Wang, B., Lai, Q., Cui, Z., Tan, T., Shao, Z., Pyrene-Degrading, A., 2008. Consortium from deep-sea sediment of the West Pacific and Its key member Cycloclasticus sp. P1. Environ. Microbiol. 10. 1948–1963.
- Wickham, H., Sievert, C., 2016. Ggplot2: Elegant Graphics for Data Analysis.
 Williams, C.J., Yamashita, Y., Wilson, H.F., Jaffe, R., Xenopoulos, M.A., 2010.
 Unraveling the role of land use and microbial activity in shaping dissolved organic matter characteristics in stream ecosystems. Limnol. Oceanogr. 55, 1159–1171.
- Yamashita, Y., Boyer, J.N., Jaffé, R., 2013. Evaluating the distribution of terrestrial dissolved organic matter in a complex coastal ecosystem using fluorescence spectroscopy. Cont. Shelf Res. 66, 136–144.
- Yamashita, Y., Kloeppel, B.D., Knoepp, J., Zausen, G.L., Jaffé, R., 2011. Effects of watershed history on dissolved organic matter characteristics in headwater streams. Ecosystems 14, 1110–1122.
- Yamashita, Y., Tanoue, E., 2003. Distribution and alteration of amino acids in bulk DOM along a transect from bay to oceanic waters. Mar. Chem. 82, 145–160.
- Yan, M.Q., Fu, Q.W., Li, D.C., Gao, G.F., Wang, D.S., 2013. Study of the pH Influence on the optical properties of dissolved organic matter using fluorescence excitationemission matrix and parallel factor analysis. J. Lumin. 142, 103–109.
- Zhang, D.-C., Li, H.-R., Xin, Y.-H., Liu, H.-C., Chen, B., Chi, Z.-M., Zhou, P.-J., Yu, Y., 2008. Marinomonas Arctica sp. nov., a psychrotolerant bacterium isolated from the Arctic. Int. J. Syst. Evol. 58, 1715–1718.
- Zhou, Z., Guo, L., 2012. Evolution of the optical properties of seawater influenced by the deepwater horizon oil spill in the Gulf of Mexico. Environ. Res. Lett. 7, 301–312.
- Zito, P., Ghannam, R., Bekins, B.A., Podgorski, D.C., 2019a. Examining the extraction efficiency of petroleum-derived dissolved organic matter in contaminated groundwater plumes. Ground Water Monit. Remediat 39, 25–31.
- Zito, P., Podgorski, D.C., Bartges, T., Guillemette, F., Roebuck, J.A., Spencer, R.G.M., Rodgers, R.P., Tarr, M.A., 2020. Sunlight-induced molecular progression of oil into oxidized oil soluble species, interfacial material, and dissolved organic matter. Energy Fuels 34, 4721–4726.
- Zito, P., Podgorski, D.C., Johnson, J., Chen, H., Rodgers, R.P., Guillemette, F., Kellerman, A.M., Spencer, R.G.M., Tarr, M.A., 2019b. Molecular-level composition and acute toxicity of photosolubilized petrogenic carbon. Environ. Sci. Technol. 53, 8235–8243
- Šantl-Temkiv, T., Finster, K., Dittmar, T., Hansen, B.M., Thyrhaug, R., Nielsen, N.W., Karlson, U.G., 2013. Hailstones: a window into the microbial and chemical inventory of a storm cloud. PLoS One 8, e53550.